The contribution of non-structural components to the overall dynamic behaviour of concrete floor slabs

Shahram Falati

New College, Oxford

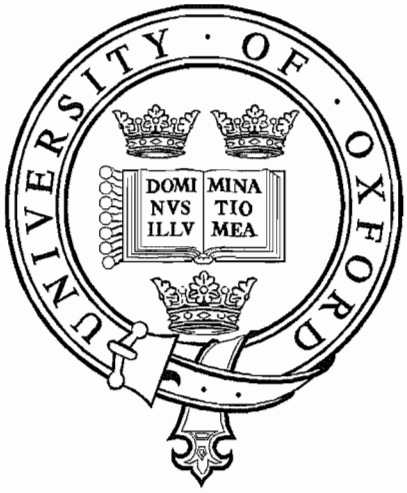

Submitted in partial fulfilment of the requirements for the degree of
Doctor of Philosophy at the University of Oxford.

Hilary 1999

To my beloved parents

Dr. Moussa Falati and

Mrs. Malaknaz Ghaemi

The contribution of non-structural components to the overall dynamic behaviour of concrete floor slabs

Shahram Falati

New College, Oxford

Submitted in partial fulfilment of the requirements for the Degree of
Doctor of Philosophy at the University of Oxford.
Hilary 1999

Abstract

Prestressing and the advent of high strength materials enable the construction of more slender floor slabs with lower values of natural frequency and damping. Under certain circumstances, the vibrations due to forcing frequencies of normal human activities can be annoying to the occupants. Since the occupants are both the source and the sensor, the vibration cannot be isolated and must be controlled by the structural system. At present, there is a limited knowledge about the overall dynamic characteristics of such concrete slabs, including contributions from individual structural and non-structural components.

An extensive programme of modal testing on a slender one-way spanning 50% scaled post-tensioned concrete slab is described. Testing was performed using electromagnetic shaker, instrummented hammer, heeldrop, and walking excitations, to determine full floor dynamic characteristics. The tests investigated the effect on vibration performance of the level of prestress, and of various non-structural additions, including vibration absorbers and effect of occupants.

It was found that an increase in prestressing force increases natural frequency and decreases damping due to closing up of microcracks. A model is presented to reflect these changes in terms of effective second moment of area. Cantilever partition tests showed energy to dissipate by swaying, and full-height partitions were seen to act as line supports leading to a significant stiffening of the slab. Analytical models are derived for both forms of partitions. Tests with false floors showed a significantly higher increase in slab damping when the floor panels rested on the pedestals, as opposed to being rigidly fixed to them. Although the addition of viscoelastic screed layers were not seen to have great effect in damping, an analytical model is derived which shows the advantage of using such layers. A TMD system was designed and installed on the floor, using plywood sheets, which led to a reduction in vibration response by as much as 80%. A theoretical model is derived to represent the TMD results and a design criterion is suggested. Finally, the effect of human-structure interaction is investigated. An analytical model shows the natural frequency of the body to be 10.43Hz with a damping of 50%. Results are also reported of tests on a full-scale field slab, confirming some of the findings of the model slab experiments.

Broadly, the results show that contrary to popular belief, merely the presence of non-structural components does not necessarily enhance the dynamic behaviour of the system. The design of these components and nature of their installation are important factors affecting their contribution to the overall floor vibrational behaviour .

Acknowledgements

I would like to express sincere gratitude and appreciation to my supervisor, Dr M.S. Williams, for his generous support and guidance throughout the duration of my research. In particular, his encouragement, useful suggestions, help and advice have been invaluable and his assistance in obtaining the experimental equipment have made this research programme possible.

The funding of the research programme and the studentship status, provided by EPSRC, is gratefully acknowledged. I am also grateful for the support and assistance of: Dr Colin Taylor of Bristol University for providing the shaker, Mr Kevin Bennett and Mr Tony Woods of PSC Freyssinet for providing the post-tensioning equipment and expertise, Dr Walter Israel of Concredamp Inc. for supplying the viscoelastic material, Tate Access Floor Systems Ltd. for providing false flooring, and Prof. Terry Jones of Oxford University for allowing me to occuppy a sizeable space at the Osney labs to conduct my year long experiments.

It has been a real privilege to be a member of Oxford University Engineering Science Department, and the Civil Engineering Group. Many people have helped me with my work at various stages and my special appreciation is extended to: Dr A. Blakeborough for unravelling the complex language of the spectrum analyser, Mr Bob Sawala for cheerfully helping out with his technical expertise and knowledge, Mrs Nicola Houliston for helping with all my administration needs and staying cheerful at all times, Prof. Guy Houlsby for his general help and advice on all matters particularly for helping with all my computing needs, Mamdouh Atia for teaching me the ins and outs of Matlab, and to Richard Thompson and Jan Mangal for making my arrival pleasant and being great friends. Also my thanks goes to Bob, Brendan, Gert, Leith, Mamdouh, Jan, Jon, Peter and Ramon, who helped me with the messy business of casting my concrete slab. Thanks also to Dave and Mark who, along with Richard, have been great office mates.

I am most honoured to have been a member of New College, Oxford. I am grateful to all the staff at the college for making my stay so enjoyable. In particular I would like to thank Dr G. Ratcliffe and Ms C. Thomas for entrusting me with the job of Junior Dean. Thanks also to Tony Beer, Peter Ryman and Vince Watley for all the entertainment and help while I was JD. Four and a half years is a long time to spend in one place and during it I have met many people and developed many strong friendships. In particular, I cannot envisage Oxford without knowing Ade Aromolaran, Mamdouh Atia, Mark Buckley, Leith Cooper, Tarek Ghaoud, Jo Knight, Ges Mannion and Steve Radcliffe, with whom I have enjoyed many adventures through the years. I also thank the following whom I met in Oxford at different times: Alan, Alun, Clare, Claus, Katia, Kitae, Lee, Liz, Marcus, Rob Wagland, Rob Taylor, Suzzanna, and many many others. I hope that our acquaintence in Oxford was only a start of a great pillar of friendship to come.

There have been many members of my family and friends outside Oxford whom have been a source of support and encouragement for me. I am most grateful to them all particularly my family members back in Iran, too numerous to mention, to whom this means as much as it does to me. Also, the loss of my dear beloved grandfather, Seyed Gholamhoussain Ghaemi, in April 1997 affected me and all my family enormously. Although he has gone to a better place, his spirit and words of wisdom will always stay with me forever.

Finally, I believe nothing in my life would have been achieved if it wasn't for the continuous support, encouragement and prayers of my parents. They have sacrificed more than many a parent for me and my brother Shahrokh, and I hope to be able to repay a fraction of their kindness during the rest of my life. It is to them that I dedicate this work.

Notation

A	Area
A_c	Cross-sectional area of concrete
A_0	Initial peak acceleration (as determined by the heeldrop test)
A_{rms}	Root mean square acceleration
A_s	Cross-sectional area of steel reinforcement
A_{st}	Steady-state acceleration
b	Width of slab
B	Structural factor
c	Viscous damping constant
c_c	Critical viscous damping constant
C_e	Dynamic crowd effect
C_x	Intermediate variable in the x-direction (Concrete Society (1993))
d	Effective depth of beam or slab
D	Flexural rigidity of a plate ($=\frac{Eh^3}{12(1-\nu^2)}$)
DAF	Dynamic amplification factor for displacement
DLF	Dynamic amplification (load) factor for acceleration
e	Eccentricity of prestressing tendons
E	Modulus of elasticity (Young's modulus)
E_c	Modulus of elasticity of concrete
E_s	Modulus of elasticity of steel
f	Frequency (Hz)
f_0	Fundamental natural frequency of a system (Hz)
f_{0j}	Fundamental natural frequency of jth component of a system (Hz)
f_{0u}	Undamped fundamental natural frequency of a system (Hz)
f_n	n^{th} linear natural frequency of a system
f_{nyq}	Nyquist frequency
f_p	Pedestrian activity rate (Hz)
f_t	Tensile stress of concrete cross-section
f_x	Natural frequency of slab in the x-direction
Δf	Frequency resolution
F	Force

F^*	Generalised force acting on a system
F_0	Force exerted by a single heeldrop (idealised as 2670N)
F_p	Force due to a single pedestrian activity
F_g	Force due to group activity
g	Acceleration due to gravity (9.81m/s^2)
G	Weight of a notional pedestrian (generally assumed as 800N)
G_d	Load density of a crowd (N/m^2)
G_{aa}	Force frequency spectrum of spectrum analyser
G_{bb}	Response frequency spectrum of spectrum analyser
G_{ab}	Cross-spectrum of G_{aa} and G_{bb}
h	Thickness of a plate, slab or beam
$H(\omega)$	Complex frequency response (FRF) of a system to applied excitation of frequency ω
H_{ab}	Transfer function (FRF) of spectrum analyser
i	integer(1,2,3,...) representing the ith harmonic frequency of a force
I	Second moment of area
I_{cr}	Cracked second moment of area of concrete slab cross-section
I_e	Effective second moment of area of concrete slab cross-section
I_t	Transformed second moment of area
I_u	Uncracked second moment of area of concrete slab cross-section
I_x	Second moment of area in the x-direction
I_y	Second moment of area in the y-direction
J	Number of discrete points in DFT
k	Stiffness of a system
k_p	Stiffness of gypsum plasterboard partition sheets
K^*	Generalised stiffness of a system
KB	DIN4150(1975) intensity of perception factor
KE	Kinetic energy
l_x	Span of one bay in the x-direction
l_y	Span of one bay in the y-direction
L	Span length
L_x	Span length in the x-direction
L_y	Span length in the y-direction
m	integer (1,2,3,...) representing m^{th} mode of vibration of a system (orthogonal to the nth mode of vibration)

M^*	Generalised mass of a system
M_a	Gross maximum bending moment
M_{cr}	Bending moment at the onset of cracking
N	Total number of harmonics of forcing frequency considered
N_x	Intermediate variable in the x-direction (Concrete Society(1993))
n	integer (1,2,3,...) representing n^{th} mode of vibration of a system
n_x	Number of bays on a floor in the x-direction
n_y	Number of bays on a floor in the y-direction
p	Loading on a system (varying with coordinates and time)
P	Impulse force due to a heeldrop (idealised as 70Ns)
P_0	AISC(1997) constant excitation force
P_t	Total prestress force due to all prestressing tendons
PE	Potential energy
q_i	i^{th} generalised co-ordinate (varying with time)
R_s	Response factor given in the SCI(1989) guide
R_x	Response factor in the x-direction (Concrete Society (1993))
R_y	Response factor in the y-direction (Concrete Society (1993))
R	Total response factor in both directions (Concrete Society (1993))
S	Stored Energy
t	Time
t_0	Time to reach first maximum amplitude in a heel impact test
t_d	Duration of a single heel impact (idealised as 0.05 seconds)
t_p	Duration of contact of feet with ground when jumping
T	Period of a signal
u	Displacement of a vibrating system (varying with coordinates and time)
$\dot{u}$	Velocity
$\ddot{u}$	Acceleration
w	Mass per unit length (=ρbh)
W	Mass per unit area
WD	Work done
W_e	Effective weight of a floor
W_t	Total weight of a floor plus contents
x, y, z	Cartesian coordinates
X_a	Force signal of spectrum analyser

X_b	Response signal of spectrum analyser
X	Amplitude of response of a system to dynamic excitation
X_{peak}	Peak amplitude of response of a system to dynamic excitation
X_I	Imaginary part of X
X_m	Modulus (magnitude) of X
X_R	Real part of X
y_t	Position of neutral axis
α_i	Fourier coefficient of the ith harmonic of forcing frequency
δ	Logarithmic decrement
Δ_b	Static deflection due to bending and shear of beam
Δ_c	Static deflection due to axial shortening of column
Δ_g	Static deflection due to bending and shear of girder
Δ_s	Total static deflection of a system
Υ_{ab}	Coherence function of spectrum analyser between force (a) and response (b)
ϕ_i	Phase lag of ith harmonic relative to the first harmonic
Φ_n	n_{th} mode shape of a system
ν	Poisson's ratio
μ	Mass ratio
∇^2	Laplacian operator
ρ	Density
σ_t	Concrete tensile strength
σ_{av}	Average prestress in slab
λ_x	Effective aspect ratio of slab in the x-direction
ω_n	n^{th} angular natural frequency of a system ($\omega_n = 2\pi f_n$)
τ	Shear stress
ζ	Damping ratio (expressed as percentage of critical damping c_c)
ζ_{eq}	Equivalent damping ratio of a structure

Contents

1 Introduction **1**

1.1 Post-tensioned floors and their vibration susceptibility 1

1.2 Overview of research needs 3

1.3 Research objectives 5

1.4 Scope of thesis 6

2 Background knowledge and literature review **8**

2.1 Introduction 8

2.2 Human perception of vibration 8

2.2.1 Vibrations and human beings 9

2.2.2 Perceptibility guidelines 10

2.3 Induced live loads on floor slabs 16

2.4 General dynamics of floor systems 19

2.4.1 Types of suspended concrete slab 19

2.4.2 Introduction to vibration of slabs 20

2.4.3 Effect of prestressing on vibration 21

2.4.4 Vibration of multiple spans or panels 22

2.5 Natural frequencies 22

2.5.1 General definitions 23

2.5.2 Theoretical background and estimation methods 23

2.5.3 Practical methods of frequency estimation 26

2.6 Damping 29

2.6.1 General definitions 29

2.6.2 Methods of structural damping measurement 31

2.6.3 Damping mechanisms in concrete 33

2.6.4 Review of measurement practice and results 35
2.6.5 Tuned mass dampers (TMDs) 36
2.6.6 Human-structure interaction 37
2.7 Floor accelerations 38
2.7.1 Estimation methods 39
2.7.2 Design guidelines 40
2.8 Remedial measures for problematic floors 43
2.9 Recent developments 45

3 Design and construction of experiment **48**
3.1 Introduction 48
3.2 Outline of tests 48
3.3 Description and design of apparatus 49
3.3.1 Instrumented impact hammer 49
3.3.2 Electromagnetic shaker 51
3.3.3 Piezoelectric accelerometers 53
3.3.4 Load cells 54
3.3.5 Spectrum analyser 54
3.4 Design of the model floor slab 55
3.4.1 Objectives of the design 55
3.4.2 Dimensions and limitations 56
3.4.3 Design of slab as a reinforced beam 56
3.4.4 Design of slab as a post-tensioned floor 57
3.4.5 Design of slab supports 58
3.5 Construction of the model floor slab 58
3.5.1 Concrete mix design 58
3.5.2 Concrete casting process 59
3.5.3 Small scale test samples 59
3.6 Additions to the floor during testing 60
3.6.1 Dead load on floor 60

3.6.2 Cantilever partitions 60
3.6.3 Full-height partitions 61
3.6.4 False flooring system 62
3.6.5 Tuned mass damper (TMD) system 63
3.6.6 Standing human 63
3.6.7 Viscoelastic screed layers 63
3.6.8 Some combinations 65
3.7 Accuracy of measurement systems 65
3.7.1 Accelerometers 65
3.7.2 Load cells 66
3.7.3 Shaker loading 67

4 Modal analysis technique and experimental procedure 68

4.1 Introduction 68
4.2 Modal analysis technique 68
4.2.1 Underlying theory 68
4.2.2 Fourier analysis of signals 70
4.2.3 Related topics in signal analysis 72
4.3 Review of modal tests on floors 73
4.4 Initial setup procedure 74
4.4.1 Location of grid points 75
4.4.2 Location of loading 76
4.4.3 Location of measurement instrumentation 76
4.4.4 Preliminary tests 77
4.5 Loading procedure 79
4.5.1 Instrumented impact hammer 79
4.5.2 Electromagnetic shaker 80
4.5.3 Heeldrop loading 80
4.5.4 Human walking 81
4.6 Measurement procedure 82

4.6.1 Natural frequencies 83
4.6.2 Phase between two points 84
4.6.3 Mode shapes 84
4.6.4 Damping ratios 85
4.6.5 Maximum accelerations 87
4.7 Small specimen tests 87

5 Experimental results **89**

5.1 Introduction 89
5.2 Concrete properties 89
5.2.1 Modulus of elasticity 90
5.2.2 Concrete cube strengths 92
5.3 Natural frequencies 93
5.4 Damping ratios 93
5.5 Mode shapes 96
5.6 Heeldrop tests 96
5.7 Acceleration responses 97
5.7.1 Excitation at resonance frequency 97
5.7.2 Walking excitation 98
5.7.3 Sensitivity analysis 100
5.8 Quality assurance tests 101

6 Analyses of results **103**

6.1 Introduction 103
6.2 Effect of prestress 103
6.2.1 Natural frequency 103
6.2.2 Damping 109
6.3 Effect of false flooring 109
6.4 Effect of non-structural partitions 110
6.4.1 Effect of full-height partitions 111
6.4.2 Effect of cantilever partitions 118

6.5 Effect of viscoelastic screed layers . . . 125
6.5.1 Screed layer properties . . . 126
6.5.2 Effect on model slab vibration . . . 126
6.5.3 General considerations and theoretical model . . . 127
6.6 Model slab accelerations . . . 131
6.6.1 Continuous vibration tests . . . 131
6.6.2 Walking vibration tests . . . 135
6.6.3 Heeldrop loading tests . . . 137

7 A simple TMD for concrete floors 138

7.1 Introduction . . . 138
7.2 Description of the proposed TMD system . . . 139
7.2.1 Effect of TMDs on floor vibration . . . 139
7.2.2 Design of the proposed plywood TMDs . . . 140
7.3 Experimental results . . . 142
7.3.1 Comparisons of TMD configurations . . . 147
7.4 Structure-TMD models . . . 150
7.4.1 Closed-form solution . . . 150
7.4.2 Numerical model . . . 152
7.4.3 Generalisation of the model . . . 156
7.4.4 Extension of the model to walking vibrations . . . 162
7.5 Sensitivity analyses . . . 164
7.6 Application of the model . . . 166
7.6.1 Proposed design guideline . . . 166

8 Human-structure interaction 168

8.1 Introduction . . . 168
8.2 Description of experiments . . . 169
8.3 Experimental results . . . 169
8.3.1 Effects on natural frequency . . . 170
8.3.2 Damping effects . . . 170

8.3.3 Effect of man at higher frequencies . . . 172
8.3.4 Summary of experimental results . . . 173
8.4 Human-structure models . . . 174
8.4.1 Undamped 2DOF model . . . 174
8.4.2 Damped 2DOF and SDOF models . . . 178
8.4.3 Sensitivity analyses . . . 180
8.5 Derivation of human body response . . . 182
8.6 Design implications . . . 185

9 Field test results **187**
9.1 Introduction . . . 187
9.2 Description of the floor . . . 188
9.3 Impact tests . . . 190
9.3.1 Instrumented hammer excitation . . . 190
9.3.2 Heeldrop excitation . . . 192
9.4 Forced vibration tests . . . 193
9.4.1 Sine-sweep loading . . . 193
9.4.2 Single sine-wave loading . . . 198
9.5 Walking tests . . . 199
9.6 Classification of the floor . . . 205

10 Conclusions **208**
10.1 Introduction . . . 208
10.2 Experimental procedures . . . 209
10.2.1 Loading apparatus . . . 209
10.2.2 Measurement apparatus . . . 210
10.3 Model slab vibration behaviour . . . 210
10.3.1 Effect of prestressing force . . . 210
10.3.2 Effect of false flooring . . . 211
10.3.3 Effect of full-height partitions . . . 212
10.3.4 Effect of cantilever partitions . . . 212

10.3.5 Effect of viscoelastic screed layers 213
10.3.6 Addition of tuned vibration absorbers 214
10.3.7 Effect of human-structure interaction 214
10.3.8 Field testing 216
10.3.9 Summary 216
10.4 Scope for further research 216

A Full experimental results **220**

B Model slab dimensions and properties **231**

C Effect of cracking on concrete section **232**

D Estimations of fundamental frequency **235**

E Derivation of gypsum partition stiffness **237**

F Example of plywood TMD design **239**

References **243**

Chapter 1

Introduction

Currently, there is a lack of knowledge about the dynamic behaviour of suspended concrete slabs. With the advent of more slender slab designs, especially with the use of prestressing, concrete floors are becoming more susceptible to vibrations. These vibrations are only a problem from a serviceability point of view. They have been encountered many times before, especially with long span floors of light construction, such as composite floors. Until now, there has been very limited research into the area of post-tensioned concrete floor vibrations, even though these types of floors can be very slender. Moreover, the knowledge of the dynamic properties of floors, particularly damping and natural frequencies, and contributions from non-structural elements is incomplete.

In this chapter, the problem of vibration susceptibility of floors to low level excitations is introduced. A brief account is presented on the merits of post-tensioned floors over ordinary reinforced slabs, and their possible drawbacks concerning vibration. The areas in which there is a need for further research are identified and the deficiencies of some current design codes are noted. The objectives and aims of the research programme are hence listed and an outline of the thesis structure is given.

1.1 Post-tensioned floors and their vibration susceptibility

Vibrations in a structure occur due to a multitude of causes, such as walking (inside a building) or wind loading (external to the building). Other forms of loading include blasts, seismic vibrations, construction loading, traffic, or human activities such as dancing and jumping [Sabnis (1979)]. While some of these vibrations can induce permanent damage, others (e.g. walking) lead to serviceability problems within the structure. Serviceability limit states in buildings are conditions in which the function of the building is disrupted because of local minor damage or deterioration of building components, or because of occupant discomfort. Vibration problems in structures are generally the most common serviceability issue faced by engineers today. Floor vibration is much

more likely to annoy people than to cause overloading or fatigue [Allen et al. (1985)]. While saftey is generally not an issue with serviceability, the economic consequences can be substantial [ASCE (1986)].

With traditional construction and design, making use of allowable or working stress criteria, serviceability usually was not a problem. Generally, simple criteria, based on percentage of span or height, dealt with cracking and motion related problems. However, changing architectural and building use requirements, coupled with improved methods of construction and design, e.g. prestressing, have led to structural systems that are less stiff and massive. In addition, the use of materials with low weight-to-strength ratios (e.g. high strength steel and concrete), has meant that modern floor areas are increasingly large with low slab thicknesses. For these flexible and lightly damped floors, serviceability issues are of paramount importance, since they are susceptible to transient vibrations induced by small impacts, such as human footfalls. Under certain circumstances, these vibrations can be very annoying to occupants of buildings [Allen (1974), Allen and Rainer (1976), Vannoy and Heins (1979), Warwaruk (1979), Murray (1981), Bachmann (1992a)]. One of the most important advances in construction design has been the advent of prestressing, which has led to more slender, and longer span, structures.

Post-tensioning, which is a form of prestressing, has been in use in floor construction for several decades, particularly in the United States, Australia, the Far East, and to some extent in Europe. Its economic and technical advantages are being increasingly appreciated, and the proportion of concrete floors being post-tensioned is growing [Khan and Williams (1995)]. Similar to normal reinforced concrete floors, post-tensioned floors can be made in flat, ribbed, one-way with beams, or waffle slab configurations (see section 2.4.1).

There are many advantages of using post-tensioning over normal reinforced concrete members. These include (i) increased clear spans, (ii) thinner slabs, (iii) lighter structures, (iv) reduced cracking and deflections, (v) reduced storey height, (vi) rapid construction, and (vii) better watertightness [Concrete Society (1994), BCA (1992)]. These advantages become most apparent when longer spans are required. Essentially, post-tensioing is an economical and fast way of achieving slender floor slabs with large open areas. The main drawback of these floors is their susceptibility to vibration. With increased spans and thinner slabs, the natural frequencies of such floors can be reduced to within the range where human annoyance due to resonance with harmonics of activities, such as walking, is likely. Furthermore, due to reduced cracking and deflections, the damping capacities of these floors are small.

Serviceability vibration problems have been encountered in many types of floors, including those of composite steel-concrete, precast, and cast-in-place construction. References relating specifically to post-tensioned, prestressed floors are very few in number [Bachmann (1992b), Waldron et al. (1993), Caverson et al. (1994), Williams and Waldron (1994)]. As these slabs become more slender with larger spans, it is logical to anticipate vibration as a problem.

1.2 Overview of research needs

A common human response to motion in buildings is that the people become anxious about the safety of the structure, even to the extent of refusing to use it. Many examples of these cases have been reported such as the closure of a new department store because of uncomfortable floor motion, or of the complete loss of secretarial efficiency in a new office building due to occupant induced floor vibration [Murray (1981)]. In such cases, the actual danger of structural collapse is very small, the strains involved often being 10 to 100 times less than those which might initiate damage [Bachmann et al. (1995)]. Nevertheless, it is a serious matter for the designer and correcting such situations is usually very difficult and expensive [Murray (1981)]. Therefore, with ever increasing numbers of flexible floors, account must be taken of the human sensitivity to vibration at the design level.

Most structural designers are acutely aware of potential floor vibration problems, but until very recently, guidelines were not available to aid in the determination of the suitability of a proposed floor system.

> "Current serviceability guidelines are not useful in many cases of new construction. The absence of meaningful criteria may be interpreted by some to mean that serviceability is not important, and encourage a casual attitude towards serviceability. With the continuing trend towards high-strength, flexible structures, efficient structural systems, and limit state design, this casual attitude will likely lead to costly problems in many buildings.... Additional research must be undertaken in numerous areas in order to develop or complete the data base needed to prepare rational and practical serviceability guidelines." [ASCE (1986)].

Increasingly, recommendations are being adopted concerning floor vibrations. SCI (1989) and AISC (1997) are two design guides specifically written for composite steel-concrete floors. For post-tensioned slabs, in recognising the need to consider vibrations, Concrete Society (1994) states:

> "Post-tensioned flat slabs usually have greater mass and a lower fundamental natural frequency than slabs on profiled metal decking. Although increasing the mass of the floor reduces the dynamic response, floors of lower natural frequency are excited by much larger components of the walking force. It is therefore likely that dynamic response will control the thicknesses of some flat slabs". [Concrete Society (1994)].

At present, there is a lack of knowledge about the means of controlling floor vibrations in terms of added stiffness and damping. Estimations of dynamic parameters can be very inaccurate. In the case of natural frequencies, a particular area of difficulty is the characterisation of boundary conditions. Also, equivalent viscous damping ratios of floors in buildings vary in a wide range depending on non-structural elements, such as hung ceilings, false flooring, furniture, partition walls, etc., and cannot be generally stated. Although the effects of architectural components have been noted in the published estimates of fundamental modal damping, [Murray (1975), CSA (1989)], only their mass is considered in the beam formula for the calculation of fundamental frequency [Pernica (1987)].

A common practice amongst designers is to pre-suppose damping values based on past experience of similar structures. This is a very crude way of measuring a major structural parameter and tests have shown that two similar buildings can have floor damping ratios which are very different [Bachmann et al. (1995)]. Hence, it is evident that the damping ratio of a complete floor system is dependent upon the damping characteristics of all its various components, both structural and non-structural. To this end, there is a need to test concrete floors in order that their dynamic behaviour may be more fully understood and the existing base of knowledge be enlarged.

> "Estimates of the stiffness, mass, and damping of building systems are needed to predict their dynamic response.... In the area of floor vibration, structural damping is an important factor in human reaction to transient vibrations that occur in lightly damped, long span floor systems. Damping depends on the level of vibration, and the contribution of non-structural elements and people. Additional field investigations of common floor systems exhibiting noticeable floor vibrations are urgently needed to determine appropriate construction systems and damping levels.... Simple and economical devices need to be developed to increase damping in floors." [ASCE (1986)].

To this end, a closer examination of vibration in concrete slabs, with specific regard to post-tensioned floors, is justified.

1.3 Research objectives

There are several very useful reports of field tests on various floor structures [Pernica and Allen (1982), Rainer and Swallow (1986), Pernica (1987), Osborne and Ellis (1990), Bachmann (1992a), Caverson et al. (1994), Pavic et al. (1994), Zaman (1996)]. However, very few laboratory experiments have been reported [Lenzen (1966), Pavic and Waldron (1996b), Pavic et al. (1997)]. While field testing provides valuable information on the behaviour of real structures, it gives little opportunity to investigate, in detail, the parameters governing vibrational behaviour, or the possible ways of improving performance. A programme of large-scale laboratory testing was therefore undertaken in this research project with the following aims:

i) to investigate the effect of the level of prestress on vibrational performance

ii) to assess the effects of various non-structural additions, including false floors and partitions, on the overall dynamic characteristics of a floor

iii) to evaluate the use of high damping admixtures, applied as layers of screed on the floor surface, in reducing floor vibrations

iv) to assess the effectiveness of tuned mass dampers (TMDs) in reducing floor vibrations and to develop a simple economical TMD in an effort to increase damping in a floor

v) to add to the understanding of human-structure interaction

vi) to investigate the most suitable and accurate method of vibration testing of real floors

vii) based on the test results, to recommend simple design guidelines for the most effective use of non-structural components on concrete floors

These objectives have been accomplished through a programme of modal testing in which a post-tensioned concrete slab strip was designed and built in laboratory conditions, at approximately 50% of full-scale. The slab was one-way spanning and simply supported, with a span to depth ratio of 38. This high slenderness was chosen deliberately so as to give a slab with a low fundamental frequency, which might therefore be expected to be prone to vibration problems. The model slab was then altered in configuration and tests were conducted with the following:

i) slab with bonded rebar only (reinforced state), with 57% of design post-tensioning force (partially tensioned state), and with full design post-tensioning force (fully tensioned state)

ii) simulated live loads applied to represent floor components such as office furniture, hospital equipment, or cars in a carpark

iii) addition of simulated cantilever partitions in three layouts

iv) addition of simulated full-height partitions in two layouts

v) addition of false flooring in two layouts

vi) addition of screed layers, treated with viscoelastic admixture, in two separate layers with differing admixture concentrations

vii) application of a simple TMD system consisting of plywood sheets, tuned with addition of known weights, in four layouts

iix) tests with the presence of one or two occupants standing stationary on the slab

The apparatus for the dynamic testing of the model slab was also designed and adapted to the specific tests. The excitations applied onto the model floor at each configuration were:

- shaker loading tests (two levels of sine-sweep and three levels of single sine wave excitations)
- instrumented hammer tests
- heeldrop tests
- horizontal walking tests
- vertical walking tests

In addition, field tests were conducted on:

i) an Edwardian building for assessment of vibration transmissibility

ii) a dance floor for assessment of vibration characterstics [Falati (1996)]

iii) an office floor for derivation of dynamic behaviour [Williams and Falati (1998)]

1.4 Scope of thesis

This thesis is restricted in scope to linear, elastic, dynamic behaviour of concrete slabs within serviceability limits. Vertical vibrations caused by regular occupancy are examined and thus the imposed excitations are of small amplitude only. Hence, it is assumed that at no stage of the research programme, damage to the model slab and inelastic structural effects have taken place. The research work and results are presented in ten chapters as described below.

The following chapter, **Chapter 2**, is a review of the current knowledge and research in the fields of human perception of vibration and the dynamic behaviour of floor slabs, in particular their natural frequency, damping, and acceleration responses. Various vibration design criteria are also presented.

Chapter 3 gives a detailed description of the dynamic testing apparatus used, including their design and construction. The design and casting process of the model concrete post-tensioned slab are also described. The latter parts of the chapter are concerned with the simulations of non-structural components on the slab, such as partitions and false floors.

In **Chapter 4**, the experimental procedure employed in the dynamic tests is explained. The chapter starts with an overview of the modal analysis technique of vibration testing, and continues to describe the use of each excitation source separately.

Chapter 5 presents the results of all the experiments for each slab configuration and **Chapter 6** describes detailed analyses of the results of prestressing effects, false floors, partitions and damping screeds. For each component, analytical model approximations are presented and compared with experimental results. Any implications are also discussed.

In **Chapter 7**, a detailed account of tests with TMDs is presented including experimental results and analyses. An analytical model is derived from which the use of the simple plywood TMD system is extended to other slab types. The chapter concludes with a proposed guideline on the use of such simple and easy-to-install systems on floors.

Chapter 8 contains a detailed account of tests conducted to assess the interaction between a floor and its occupants. Simple models are derived, which show that the current treatment of human-structure interaction in the design codes is incomplete.

An account is given in **Chapter 9** of a field test conducted to assess the dynamic characteristics of an office floor. The experimental procedure is presented and the results are analysed. The floor is then classified for its vibration perceptibility.

Finally, **Chapter 10** lists the conclusions of the research programme, describes its main findings, and gives possible recommendations for future work.

Chapter 2

Background knowledge and literature review

2.1 Introduction

Vibration tests on slender suspended long span floors have been ongoing since the early 1950s, when serviceability problems were encountered with annoying vibrations of some slabs. Although some design guides mention floor vibrations as a serviceability design concern [DIN4150/2 (1975), BS6472 (1984), NBCC (1985), CSA (1989), ISO2631/2 (1989), SCI (1989), Concrete Society (1994), AISC (1997)], there are others that simply rely on limiting deflection values or span-depth ratios to control the problem [ACI (1995), ACI-ASCE (1974), FIP (1980), Freyssinet (1994)]. This approach would be adequate for stiff, heavy systems of the past, but is sometimes found to be unsuitable for slender, long span floors of recent years.

In this chapter, a detailed review of research on human perception of vibrations and floor dynamics is presented, including representations of typical live loads in buildings. In particular, various methods of estimating floor responses and the modal parameters of natural frequency and damping are described and the various vibration serviceability guidelines are presented.

2.2 Human perception of vibration

The human body can sense vibration displacement amplitudes as low as 0.001mm, whilst fingertips are 20 times more sensitive [Bachmann et al. (1995)]. Human perception of vibration is very complex and depends on many inter-related factors, such as the person's posture and level of concentration. The following is a review of current knowledge in this field and the development of criteria for

acceptability of vertical floor vibrations.

2.2.1 Vibrations and human beings

There are three main types of human exposure to vibration:

- vibrations applied to the whole body surface (e.g. high intensity sound)
- vibrations applied to particular parts of the body (e.g. to hands by an electric drill)
- vibrations which are transmitted to the body as a whole through the supporting surface (e.g. from floor to feet of a standing person)

It is also possible for an indirect vibration nuisance to be caused by the vibration of external objects in the visual or aural field (e.g. rattling of windows). The response of the person to the vibration is mainly dependent on:

- type and intensity of excitation (e.g. impulsive shock, machinery vibration, etc.)
- distance from the source and the duration of vibration
- place and frequency of occurrence, time of day, and expectancy level
- body orientation and posture (standing, sitting, lying down, stiff, relaxed, etc.)
- personal activity (resting, walking, running)
- other factors (e.g. age, sex, level of concentration, sharing of experience with others, etc.)

Man is sensitive to mechanical oscillations ranging in frequency from below 1Hz up to at least 100kHz. This range of sensitivity is much broader than the range of human hearing [Guignard (1971)]. Oscillations at the lowest frequencies of around 0.1-3Hz are characteristic of large artificial structures which may transmit vibration to man (e.g. tall buildings or long suspension bridges). The range from about 3-30Hz is characteristic of 'vibration' in the everyday sense, occurring in vehicles, buildings or near machinery. It is also the range in which vibration is induced in many building components such as walls, floors and house frames. Such vibration may also be caused by disturbances within the building itself, including footfall. At frequencies much above 30Hz, typical of the response of lighter building elements such as windows and room fittings, sensitivity to vibration merges with and generally becomes secondary to the response to audible noise.

Human response to vibration and its influence on a person's performance has been widely studied using both subjective and objective methods [Grether (1971), Guignard (1971)]. Many studies

have been very narrowly focused on a particular form of transport or a particular aspect of human response, such as visual impairment. Also, much of the published work has been concerned with relatively intense and continuous vibration, such as is felt in vehicles or industrial machinery.

A common approach has been to use subjective experiments as a guide to tolerable exposure levels. A typical graph from such an investigation is shown in figure 2.1, where it can be seen that maximum sensitivity occurs at around 4-8Hz. This agrees with research, which has established whole body resonance in this range [Dieckmann (1958), Herterich and Schnauber (1992), Fairley and Griffin (1989)]. As is usually the case, the vibration amplitude in figure 2.1 is given as an acceleration, expressed as a fraction of the acceleration due to gravity, (g). The lines in the figure indicate acceptability limits, where the region above a line denotes unacceptable vibrations. The direction of the motion relative to the human body is significant and in the case of vibrating floors, vertical vibrations are most prominent.

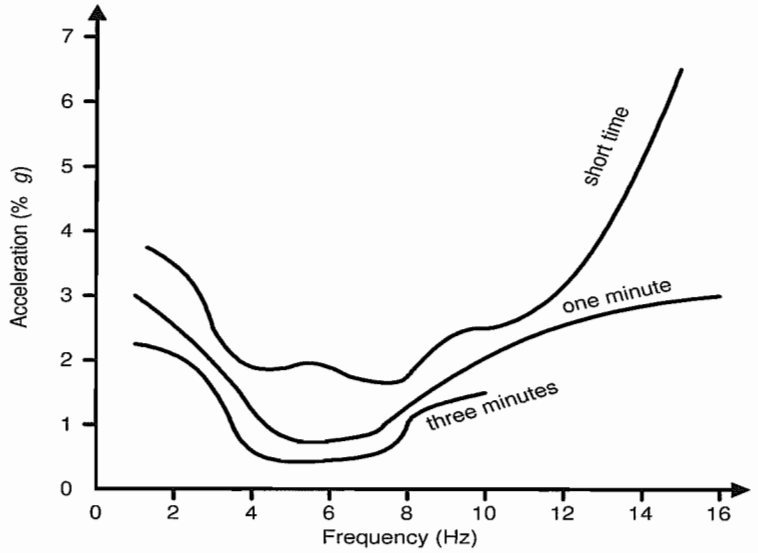

Figure 2.1: Magid et al(1960) human subjective tolerance to whole body vertical sinusoidal vibrations [from Grether (1971)]

2.2.2 Perceptibility guidelines

In this section, attention is focused on the perception of vibration by occupants of buildings, in particular long span floors. As this is a comparatively recent problem, it is not addressed fully in many design codes, but certain guidelines have been proposed which will be reviewed.

Here, a common representation of the various plots is adopted, as the guidelines proposed by each source vary widely using different axes and units. In the following discussion, each source's original

graph is converted into the common graphical representation (CGR) of metric root mean square (RMS) acceleration versus frequency. The CGR is consistent throughout with the ISO/BSI/ANSI scales and some suggested limits, as marked on the graphs. These scales and limits are discussed later in this section. Each line shown on the graphs represents a constant level of human reaction and is known as an iso-perceptibility line. The area above any line represents a reaction greater than the area below. Caverson (1992) used CGR with peak accelerations versus frequency.

The first comprehensive research on human sensitivity to vibration was carried out by Reiher and Meister (1931). They subjected a representative group of people to vertical and horizontal vibrations of five minutes duration. The amplitudes and frequencies of vibration were varied and the subjects rated the motion in one of six categories: *imperceptible, slightly perceptible, distinctly perceptible, strongly perceptible, disturbing* or *very disturbing.* The CGR plot of their results for vertical vibration are shown in figure 2.2. Note that damping is not mentioned in these investigations and that the duration of the vibrations is long enough to be regarded as continuous, rather than transient, excitation. The limits above *distinctly perceptible* are not included in figure 2.2 as they fall above serviceability conditions.

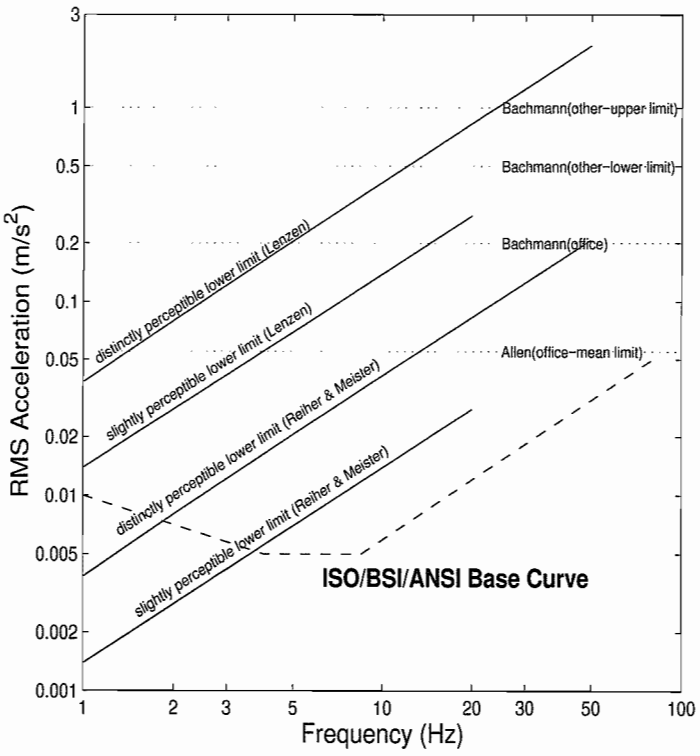

Figure 2.2: CGR of Reiher-Meister(1931) and Lenzen(1966) modified Reiher-Meister

Perhaps the first study to address human perception of floor vibrations in particular, was carried out by Lenzen (1966). He identified the main source of floor vibration as the occupants themselves impacting the floor through normal usage. As a result, he modified the Reiher-Meister graphs by scaling the amplitude axis up, by a factor of ten, to account for the reduced human sensitivity to transient vibrations, figure 2.2. Citing results from several floor tests, Lenzen concluded that if damping reduces the vibration to a negligible quantity in five cycles, the human would not respond, whereas if it persists beyond 12 cycles, he will respond as if to steady-state vibrations.

DIN4150/2 (1975) (as reported by Bachmann et al. (1995)) was one of the first design codes to consider structural vibrations. The limits given are based on a parameter known as the *intensity perception factor* (KB), which is calculated empirically in terms of frequency and displacement and is applied to frequencies within the range 1-80Hz. The formula for KB is shown in equation 2.1 in terms of peak acceleration, A_0, and its CGR in shown in figure 2.3. In using these codes, a designer would have to ensure the calculated value of KB falls below the limits of table 2.1.

$$KB = \frac{0.8f^2}{\sqrt{(1+0.032f^2)}} \cdot \frac{A_0}{4\pi^2 f^2} \tag{2.1}$$

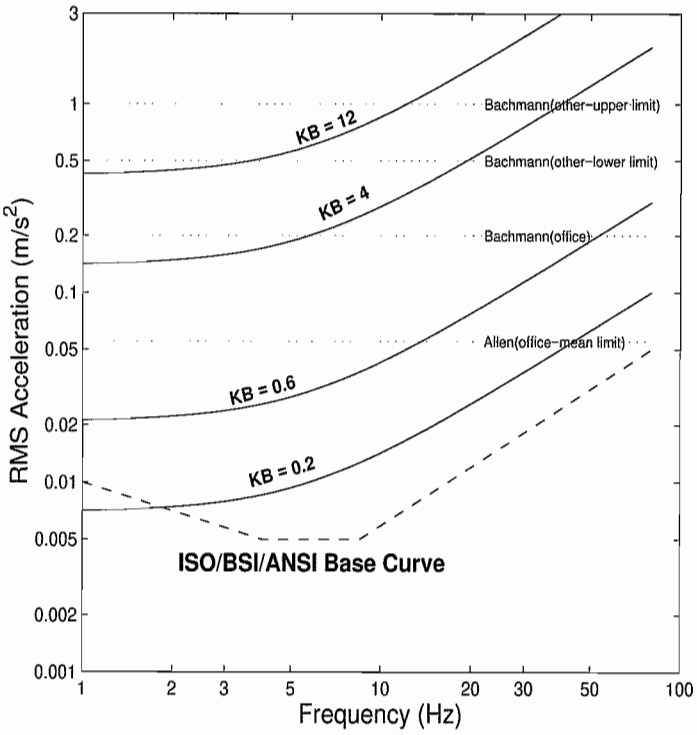

Figure 2.3: CGR of German standard DIN4150/2 (1975) perceptibility graph

Table 2.1: DIN4150/2 (1975) acceptable KB values for buildings [after Bachmann et al. (1995)]

Building type	Time	Continuous or intermittent vibration	Transient vibration (several occurrences per day)
rural, residential and holiday resort	day	0.2	4.0
	night	0.15	0.15
small town and mixed residential	day	0.3	8.0
	night	0.2	0.2
small business and office premises	day	0.4	12.0
	night	0.3	0.3
industrial	day	0.6	12.0
	night	0.4	0.4

Following tests on 42 slabs, Allen and Rainer (1976) proposed a vibration criterion for long span floors, which was incorporated into CSA (1989). The data for each test floor included initial amplitude from a heeldrop impact (see section 2.7.1), as well as frequency, damping ratio, and subjective evaluation by occupants. By correlating their results, they arrived at a continuous and walking vibration criterion, the CGR of which is shown in figure 2.4. The continuous vibration iso-perceptibility line is due to a person walking, who causes between 10 and 30 cycles of vibration. One limitation of the criterion is that it can only be applied to quiet occupancies (i.e. residential, school and office floors), whereas the scales given in DIN4150/2 (1975) take account of the usage of the structure. Pernica and Allen (1982) modified the criterion from quiet to active occupancies by increasing the limits by a factor of three to account for usage such as shopping centres or carparks.

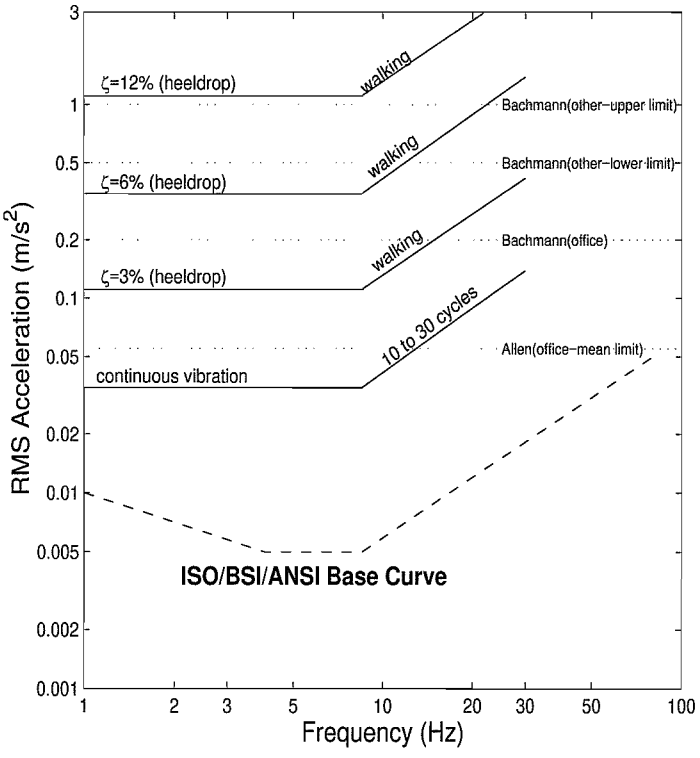

Figure 2.4: CGR of Allen and Rainer (1976) and CSA (1989) annoyance criteria for floor vibrations

The International Standards Organisation (ISO) revised its design codes concerning vibrations in 1985 [ISO2631/1 (1985)] and again in 1989 [ISO2631/2 (1989)] in order to encompass a broader review of motion in structures within the frequency range of 1-80Hz. These codes apply to vibrations in both vertical and horizontal directions and deal with random and shock, as well as harmonic excitations. The guideline is very similar to [BS6472 (1984)] and [ANSI S3.29 (1983)]. These guidelines differentiate vibrations into three distinct catergories:

continuous excitation: steady-state excitation induced by machinery, etc. with typically more than 30 cycles of vibration.

intermittent vibration: lasts a few seconds but is characterised by a build-up to a level that is maintained for several cycles of vibration. Examples include traffic vibration and humans walking across a floor.

transient excitation: characterised by a rapid build-up to a peak followed by a decay. Examples include blasting or human jumping on a floor.

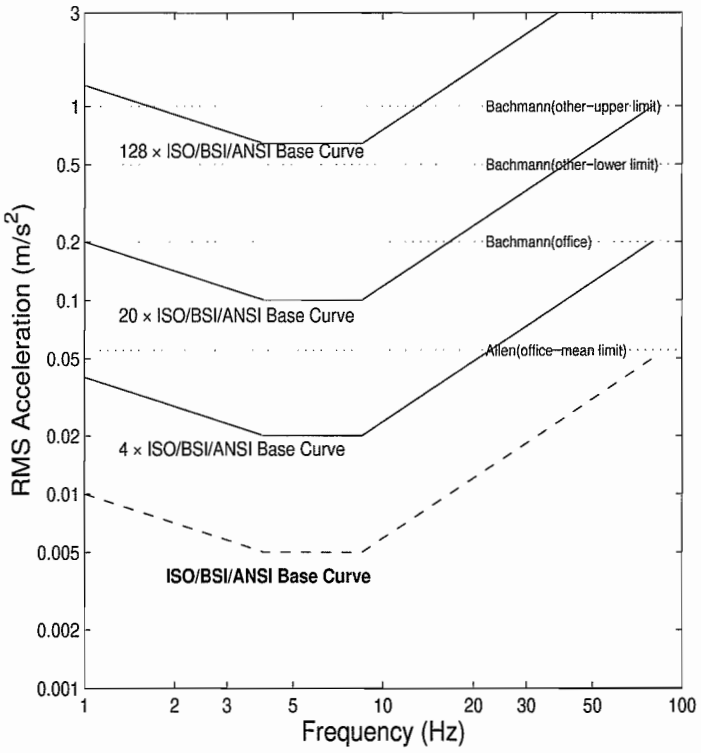

Figure 2.5: CGR of ISO2631/2 (1989), BS6472 (1984) and ANSI S3.29 (1983) building vertical vibration curves

The CGR form of the three guides is given in figure 2.5. There is a base curve which applies to floor vertical vibration of a person standing or sitting. This is the boundary at which the comfort level of a person starts to reduce as a result of vibrations (commonly known as *reduced comfort*

level base curve). This base curve can be adjusted by applying a weighting factor to the allowable accelerations. Variations in this weighting factor account for the type of excitation, occupancy, and the time of day. Table 2.2 shows these weighting factors for the various conditions.

Table 2.2: ISO/BSI/ANSI recommended Base Curve weighting factors

Place	Time	Continuous or intermittent vibration	Transient vibration (several occurrences per day)
critical working areas	day or night	1	1
residential	day night	2 to 4 1.4	60 to 90 20
office	day or night	4	128
workshop	day or night	8	128

Following several experiments on concrete floor slabs, Waldron et al. (1993) and Caverson et al. (1994) assessed various acceptability criteria and discussed the ways in which the guidelines, drawn normally for composite slabs, could be applied to post-tensioned suspended concrete floors. They concluded that many of the scales of human perception of vibration are very similar in form, but they can yield different results because of small numerical differences in the borderline regions. However, these scales are seen to be difficult to use in design because of the need to calculate the frequency and acceleration response of slabs to human activities.

Bachmann and Ammann (1987) argued that due to the lack of exact knowledge about various floor parameters and their inter-relations, and also because of lack of simple design methods, it would be more practical to have limits by which engineers can design various floors. They presented acceleration limits based on past experience and measured values of similar structures. The use of acceleration limits has also been described by others [Ellingwood and Tallin (1984), Allen (1990b)], as shown in table 2.3. These are plotted in figures 2.2 to 2.5 and are seen to be generally quite high compared to the other guidelines. Also, there is a high degree of varability in the suggested acceleration limits, particularly for sensitive environments, such as offices.

Table 2.3: Suggested RMS acceleration limits (m/s^2)

Structure type	Bachmann(1987)	Allen (1990b)	Ellingwood(1984)
pedestrian structures	0.5-1.0	-	0.5-2.0
office buildings	0.2	0.04-0.07	0.5
gymnasia & sports halls	0.5-1.0	0.4-0.7	-
dancing and concert halls	0.5-1.0	0.4-0.7	-

In summary, the human perception to vibrations is very complex and depends on many factors. Most perceptibility scales can reasonably predict human response given an accurate definition of the vibration, though some uncertainties and inconsistencies still remain. The difficulty arises at the design stage, where predicting the vibration characteristics is uncertain, as discussed in the subsequent sections. Some recent codes of practice, [BS6472 (1984), ISO2631/2 (1989) and DIN4150/2

(1975)], introduced weighting factors, used to make the design more conservative according to the activity and the type of occupancy. Presently, this is the most commonly used approach.

2.3 Induced live loads on floor slabs

In this section, the knowledge on the forces induced by human activity on floors is reviewed. Live loads are imposed on structures by use and occupancy. Serviceability design in most building codes is based on statically applied live loads and aims to limit cracking and deflection. As such, vibrations and time-varying occupant induced loads have not normally been considered.

There are a number of possible causes of dynamic excitation on floors. It is widely accepted that continuous vibrations caused by machinery, road and rail traffic, or wind, should be dealt with at the design stage. Forces exerted by human activities on a floor are more difficult to design against. The loading induced by human movements may be categorised as static, impulsive or continuously changing, depending upon the duration in which a motion is achieved. Impulsive loads may be caused by motions such as a jump, dropping into a seat, or stopping suddenly. Movements such as walking, swaying, or rhythmic jumping, generate intermittent or continuous loading.

Perhaps the most universal human-induced excitation is the effect of walking on the floor. Walking is complex to represent mathematically as it involves the parameters of amplitude and position, both time-dependent, and the fact that people walk in different ways. Several studies of forces exerted by normal walking have been conducted [Wheeler (1982), Ellingwood and Tallin (1984), Mouring and Ellingwood (1994), Ebrahimpour et al. (1996)]. The starting point in developing an accurate model is the representation of the force due to a single human footfall. Footfall forces measured during several different walking activities were evaluated by Wheeler (1982) and are shown in figure 2.6. He found that the pacing frequency ranged between 1.7Hz and about 3.2Hz, from slow walking to running respectively. In terms of velocity, a slow walker travels at around 0.75m/s, a fast walker at about 1.75m/s, beyond which a person breaks into jogging and then running.

Walking as an activity is characterised by the heel and toe contact peaks and by the overlapping of succeeding paces; figure 2.6 shows an overlap of approximately 0.1 seconds for normal walking. Since the loading is periodic, it can be represented by a Fourier series of the form:

$$F_p(t) = G\left\{1.0 + \sum_{i=1}^{N} \alpha_i \sin\left(2\pi i f_p t - \phi_i\right)\right\} \tag{2.2}$$

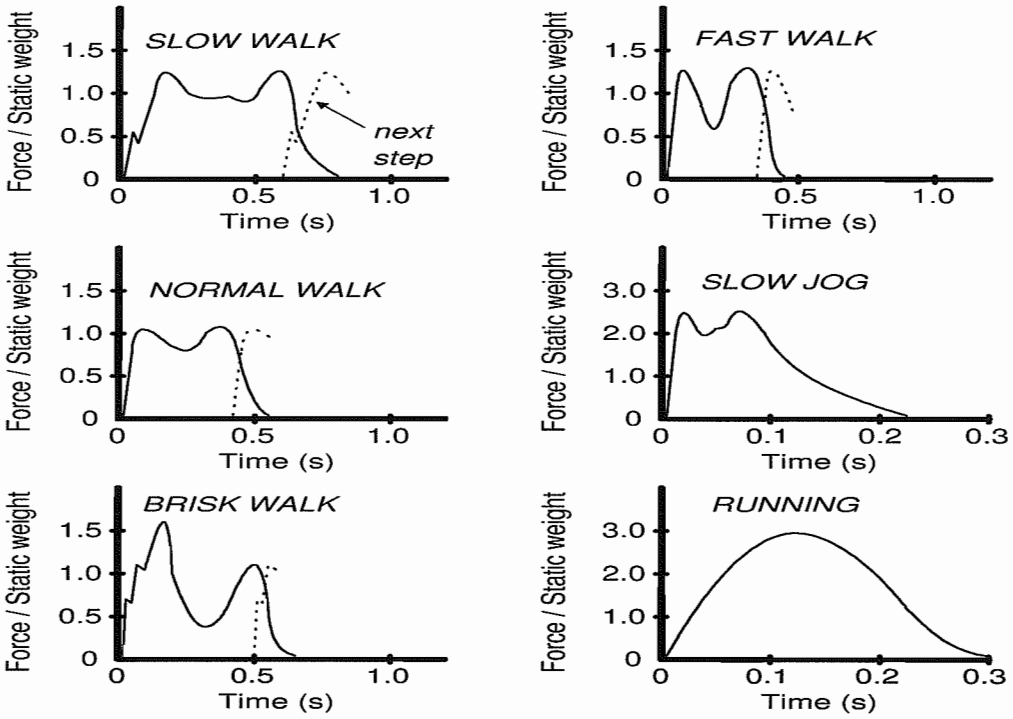

Figure 2.6: Pedestrian force-time histories [after Wheeler (1982)]

where G is the weight of the person, α_i is the Fourier coefficient of the ith harmonic and N is the total number of contributing harmonics. Usually, a reasonable approximation can be obtained using three to six Fourier terms [Allen et al. (1985), SCI (1989), Mouring and Ellingwood (1994), Ji and Ellis (1994a), Bachmann et al. (1995), Ebrahimpour et al. (1996)]. Values of the Fourier coefficients have been calculated analytically for different contact ratios [Ji and Ellis (1994a)], or have been derived experimentally for different activities [Bachmann et al. (1995), Ebrahimpour et al. (1996)]. Typical measurements are shown in table 2.4.

Table 2.4: Bachamnn et al(1995) normalised dynamic forces of human activities

Type of activity	**Activity rate (Hz)**		**Fourier coeffs & phase lag**					**Design density (persons/m^2)**
			α_1	α_2	α_3	ϕ_2	ϕ_3	
walking (continuous ground contact)	vertical	2.0	0.4	0.1	0.1	$\pi/2$	$\pi/2$	~ 1
		2.4	0.5					
	forward	2.0	0.2	0.1				
running (discontinuous ground contact)		2.0-3.0	1.6	0.7	0.2			-
jumping (simultaneous ground contact of both feet)	normal	2.0	1.8	1.3	0.7	$\star$	$\star$	$\sim$ 0.25-0.5
		3.0	1.7	1.1	0.5	$\star$	$\star$	
	high	2.0	1.9	1.6	1.1	$\star$	$\star$	$\star \rightarrow \phi_2 = \phi_3 =$
		3.0	1.8	1.3	0.8	$\star$	$\star$	$\pi(1 - f_p t_p)$
dancing (equivalent to brisk walking)		2.0-3.0	0.5	0.15	0.1			$\sim$ 4-6

As the frequency of walking increases, a threshold is reached where the activity is no longer classified as walking, but as jogging or running. In these modes, no more than one foot is in contact with the floor at any time and there is no separate heel and toe contact. As a result, the force-time graph

consists of near-sinusoidal peaks, as shown in figure 2.6. The running and jumping cases constitute the most severe loadings, as can be seen from the high values of α_i in table 2.4.

Recently, researchers have considered the effect of groups of people walking about a floor at random [Ellingwood and Tallin (1984), Allen and Murray (1993), Mouring and Ellingwood (1994), Ebrahimpour and Fitts (1996)]. Generally, the excitation lacks coherence unless the group is walking in step and so a single pedestrian footfall provides an appropriate excitation amplitude for research purposes. However, in situations such as lively music concerts or aerobics, dynamic loads will be significant when any crowd movement (dancing, jumping, rhythmic stamping) is synchronised. In such cases, equation 2.2, describing the load, F_p, due to one person, can be replaced by the load due to a group, F_g: [BRE 426 (1997)]

$$F_g(t) = G_d \left\{ 1.0 + C_e \sum_{i=1}^{N} \alpha_i \sin\left(2\pi i f_p t - \phi_i\right) \right\} \tag{2.3}$$

Here, the weight of one person, G, is replaced by the load density of the crowd, G_d, and the factor C_e is introduced to represent the dynamic crowd effect, accounting for the fact that the crowd movement will not be perfectly synchronised [Ji and Ellis (1993)]. Although problems relating to crowd events had been recognised for many years, the first mention of such loading in British codes was in BS6399 (1996), relating to loads produced at pop concerts [Ji and Ellis (1997)].

Much larger impulsive loading can arise as a result of the heeldrop test. This is performed by a person of average weight (≈800N) rising to the balls of his feet (≈60mm from the floor), and then suddenly droping his weight on his heels striking the floor. The standard graphical approximation of a heeldrop is shown in figure 2.7, with an initial peak load of 2.67kN and a duration of 0.05 seconds [Lenzen (1966), Murray (1975), Allen et al. (1979), Becker (1980)]. Its relative simplicity and ease of use as a standard and practical method has meant that many researchers have relied on heel-impact in their experiments, including for derivation of some human perceptibility guidelines [Lenzen (1966), Murray (1975), Allen and Rainer (1976), Wiss and Parmelee (1974), Foschi et al. (1995), Becker (1980)]. However, while the test may be meaningful for evaluating the response of floor systems to activities that cause impact forces, it produces an isolated transient vibration, which is not a good simulation of vibrations due to walking [Ellingwood and Tallin (1984), Onysko (1986)]. Furthermore, the heel-impact test indicates a stronger dependence on damping than has been found in other cases.

In summary, there are three main sources of human-induced loading. The most common is walking, which depends on many factors such as position on floor, stride length, step duration, and type of footfall function. These are functions of the pacing frequency and vary from person to person.

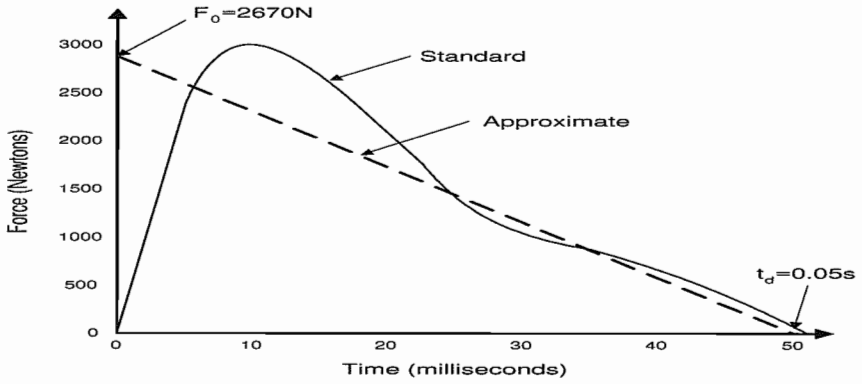

Figure 2.7: Approximation of heeldrop loading

Jogging and running are footfall activities, with the difference that at no point are both feet touching the ground. In some cases, dancing and jumping have similar representations to running and jogging, however, when a group is involved there is a likelihood of coherence of imposed forces. Factors to be considered here include the number of participants, the intensity of activity, and the positioning of the people with respect to each other. Impulsive loading is best represented by the heeldrop test, which depends on factors such as weight of the person and the duration of loading.

2.4 General dynamics of floor systems

Whether the loadings described in section 2.3 will cause unacceptable vibrations will depend on the dynamic characteristics of the floor system, particularly its natural frequency and damping. These parameters, and methods of their estimation, are discussed in subsequent sections. In this section, some general comments on post-tensioned floor types, and their dynamic behaviour, are given.

2.4.1 Types of suspended concrete slab

Post-tensioned concrete slabs are generally long span, slender structures which can be of many types, as shown in figure 2.8. Slabs are generally designed as either one or two-way spanning, depending on the way in which the floor load is to be transferred to the supports. Of the slab configurations in figure 2.8, ribbed and continuous band beam slabs are one-way spanning, because the load is principally supported by bending of the slab in one direction, perpendicular to the direction of bending of beams. Flat slabs, waffle slabs, or slabs with beams in two directions, behave as two-way systems. Note that the category of the slab (one or two-way spanning) is a

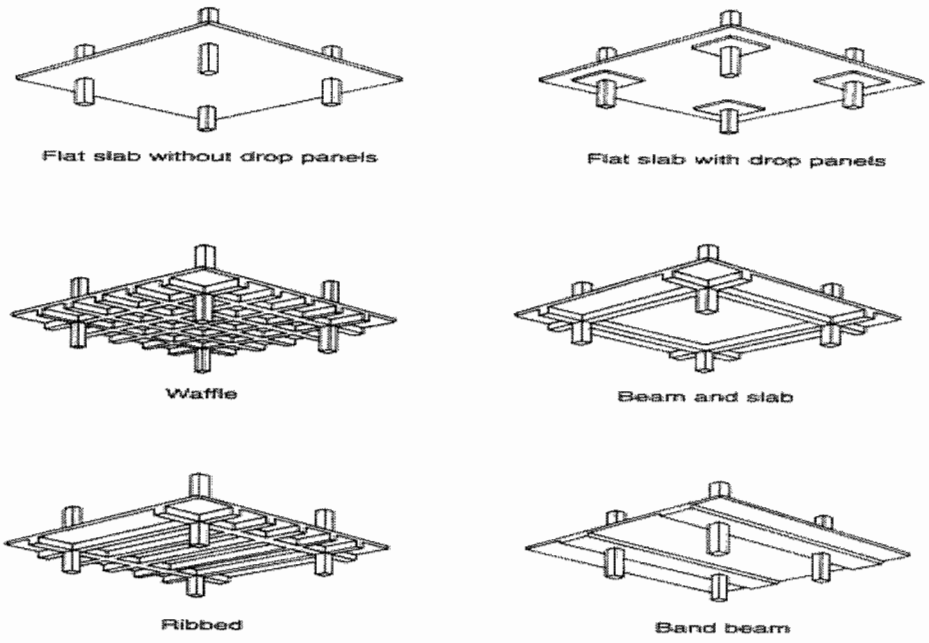

Figure 2.8: Types of suspended concrete slabs (from Khan and Williams (1995))

design assumption and the actual behaviour, static or dynamic, may deviate significantly from this.

2.4.2 Introduction to vibration of slabs

Insight into the vibration of floor slabs can be gained by considering the dynamic characteristics of simple beams and plates. A continuous element, such as the simply supported beam of figure 2.9, will have a series of natural frequencies, each associated with its own mode shape. So long as behaviour is linear, the various modes are dynamically independent and response can be synthesised by adding modal solutions computed independently. The lowest frequency mode is known as the fundamental and the higher modes have shapes of increasing complexity.

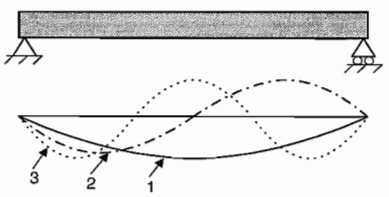

Figure 2.9: First three mode shapes for a simply supported beam

A useful insight into the behaviour of floor slabs is given by the behaviour of an orthotropic plate, shown in figure 2.10. The fundamental mode shape resembles the corresponding beam mode shape

in both directions, and this principle also applies to the higher modes. If the stiffness is highly orthotropic, the weak direction deformation has relatively little effect on the frequency and a basic family of modes retaining the fundamental shape in the strong direction is observed. One-way spanning slabs, such as beam-slab floors, behave in this way. Two-way slabs exhibit more isotropic behaviour. The vibration characteristics of such slabs are more complex and, for most boundary conditions, exact solutions of their natural frequencies and mode shapes are not available [Szilard (1974)]. It should be noted, however, that given the correct boundary conditions and material properties, the finite element (FE) method of analysis will estimate these parameters closely. The FE method is not used in this work but its merits are discussed in section 2.9.

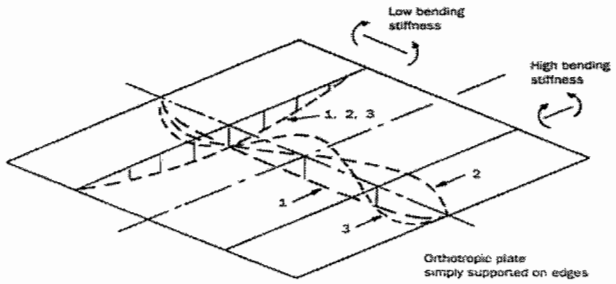

Figure 2.10: Modeshapes of orthotropic plate (from SCI (1989))

2.4.3 Effect of prestressing on vibration

There is at present some doubt about the effects of prestressing on the dynamics of a system. Conventional analysis suggests that an axial load, applied along the centroidal axis of a beam, affects its vibration characteristics, since additional out-of-balance forces are generated as the beam deflects (see figure 2.11(a)). In a prestressed member, however, the load moves with the beam and no out-of-balance moments arise (see figure 2.11(b)). Therefore, the natural frequencies and mode shapes would be expected to remain unchanged, see section 6.2.

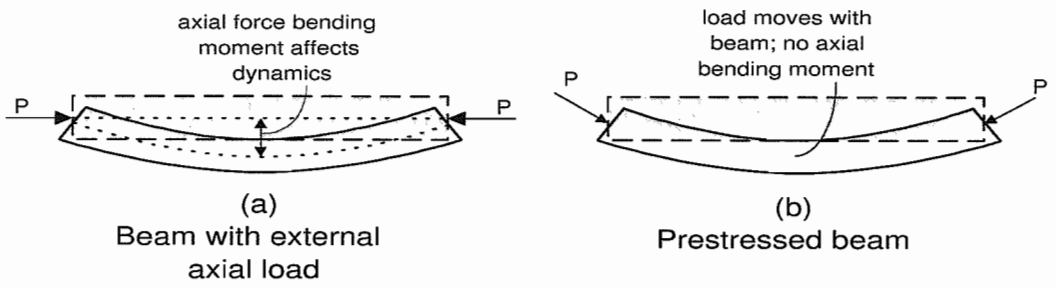

Figure 2.11: Effect of prestressing on beam vibration

Nevertheless, in practical cases, small increases in natural frequency are observed as a result of prestressing. In a reinforced beam, the concrete acts only in the area of the cross-section that is in compression, and would be cracked in the tension zone. In a prestressed beam, prestressing force imposes pre-compression in the tension zone so that, in most cases, the entire cross-section remains uncracked and elastic. This leads to a difference in stiffness between a normally reinforced and prestressed concrete element of similar geometry, due to the difference in the effective second moment of area. This in turn depends on the amount of cracking present in the section. Therefore, due to fewer cracks and greater effective section, it is likely that any prestressed member would be stiffer than one similarly reinforced, hence resulting in higher natural frequency. This theory is widespread among researchers [Dall'Asta and Dezi (1996), Deák (1996)], but yet to be fully proven.

2.4.4 Vibration of multiple spans or panels

For continuous floors, such as the one shown in figure 2.12, it is generally expected that the adjacent panels move in opposite directions (i.e. out of phase) when vibrating. The inertial forces due to the vibrations act in the senses shown and enhance the deflections. For static design, however, the self-weight effects of adjacent spans combine to reduce the corresponding stresses and deflections.

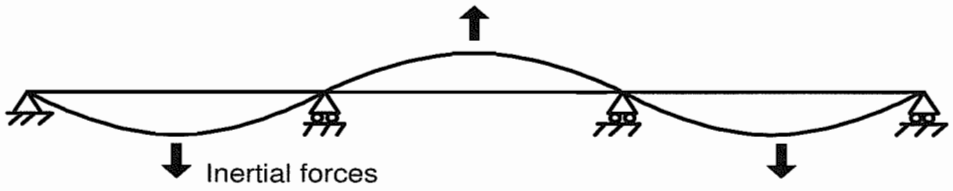

Figure 2.12: Fundamental mode shape of a continuous beam

2.5 Natural frequencies

The natural frequency of a floor slab is a key parameter in defining its dynamic behaviour. Concrete slabs are three dimensional and redundant in nature, making their behaviour complex and the theoretical estimation of their fundamental properties daunting. A particular area of difficulty is the accurate characterisation of the boundary conditions. In general, a floor is simplified theoretically and then its behaviour interpreted. In practice, this simplification is carried out in the design guides, where usually approximate formulae for the estimation of natural frequency and floor response, based on beam theory, are given. In the following sections, theoretical and practical approaches for evaluating floor natural frequencies are given, and the various methods are discussed.

2.5.1 General definitions

The simplest model of a dynamic system has one degree of freedom and is characterised by a mass, m, supported by a spring with stiffness, k. The undamped fundamental natural frequency of such a system is given by:

$$f_{0u} = \frac{1}{2\pi}\sqrt{\frac{k}{m}} \tag{2.4}$$

Taking the static deflection due to the self-weight of the mass, $\Delta_s = \frac{mg}{k}$, this can be written as:

$$f_{0u} = \frac{1}{2\pi}\sqrt{\frac{g}{\Delta_s}} \tag{2.5}$$

In real systems, any oscillations will cease with time, due to the dissipation of energy. This vibration decay, known as *damping*, is assumed to develop a force that opposes the direction of motion. The fundamental damped natural frequency of a SDOF system is:

$$f_0 = f_{0u}\sqrt{1-\zeta^2} = \frac{1}{2\pi}\sqrt{\frac{k}{m}(1-\zeta^2)} = \frac{1}{2\pi}\sqrt{\frac{g}{\Delta_s}(1-\zeta^2)} \tag{2.6}$$

where ζ is the damping ratio (see section 2.6 for a fuller definition of damping). The following sections describe the theory involved in calculating the natural frequencies of more complex systems.

2.5.2 Theoretical background and estimation methods

Vibration of a beam

Consider a simply supported beam with a mass per unit length $w = \rho A$, where ρ is density and A is cross-sectional area. By taking an infinitely short elemental length of beam, figure 2.13, and applying Newton's second law of motion, the partial differential equation of motion of the beam can be obtained: [Rao (1995)]

$$\frac{\partial^2}{\partial x^2}\left(EI(x)\frac{\partial^2 u}{\partial x^2}\right) + w\frac{\partial^2 u}{\partial t^2} = p(x,t) \tag{2.7}$$

For unforced free vibration, separation of variables can be used by assuming a solution in the form $u(x,t) = \Phi(x)T(t)$. The resulting natural frequencies and corresponding mode shapes are:

$$f_n = \frac{n^2\pi}{2}\sqrt{\frac{EI}{wL^4}} \qquad \text{and} \qquad \Phi_n(x) = C_n \sin\left(\frac{n\pi x}{L}\right) \tag{2.8}$$

where n is the order of natural frequency and C_n is an arbitrary mode shape amplitude factor. There are infinite numbers of frequencies and orthogonal mode shapes and, so long as motion is linear, any deflected shape is the sum of these modes. Figure 2.9 shows the first three modes.

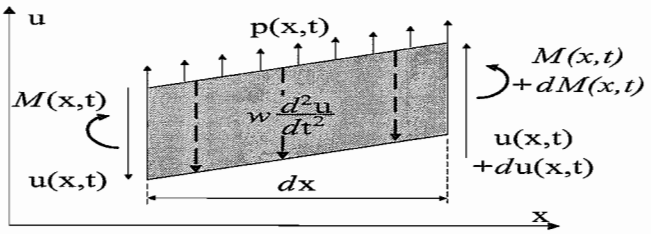

Figure 2.13: Vibrating beam element

Vibration of a plate

A differential equation for the motion of a plate can be derived as in the case of the beam by adding an extra dimension. For a rectangular plate with mass per unit area, W, simply supported on all four edges, the equation of motion is [Szilard (1974)]:

$$D\nabla^2\nabla^2 u(x,y,t) = p(x,y,t) - W\frac{\partial^2 u(x,y,t)}{\partial t^2} \tag{2.9}$$

where $D = \frac{Eh^3}{12(1-\nu^2)}$ is the flexural rigidity of the plate and ∇^2 is the Laplacian operator. For free vibration assume a solution of the form $u(x,y,t) = X(x)Y(y)T(t)$, where the time function $T(t)$ is sinusoidal and $\Phi(x,y) = X(x)Y(y)$ is a double Fourier series. The natural frequencies are:

$$f_{mn} = \frac{\pi}{2}\left(\frac{m^2}{L_x^2} + \frac{n^2}{L_y^2}\right)\sqrt{\frac{D}{W}} \tag{2.10}$$

These results can be interpreted as earlier in section 2.4.2 for an orthotropic plate. For more complex boundary conditions and shapes, exact solutions are not readily available [Szilard (1974)].

Rayleigh's principle

This method provides a means of estimating an upper bound to the fundamental frequency of a system. It is based on energy concepts and states that the maximum kinetic and potential energies of a system are equal. The method is particularly useful for systems with many degrees of freedom. Consider a vibrating beam whose fundamental mode shape can be fully described by $\Phi(x)$. By assuming the motion of the beam to be described as $u(x,t) = \Phi(x)\cos\omega t$, the maximum kinetic and potential energies associated with this motion are: [Rao (1995)]

$$KE_{max} = \frac{\omega^2}{2}\int_0^L \rho A(x)(\Phi(x))^2 dx \tag{2.11}$$

$$PE_{max} = \frac{1}{2}\int_0^L EI(x)(\Phi''(x))^2 dx \tag{2.12}$$

Assuming conservation of energy (i.e. no damping), the maximum energies can be equated resulting in an estimate of the fundamental frequency, once the deflection $\Phi(x)$ is known. Generally, the

static equilibrium shape is assumed for $\Phi(x)$. However, it should be noted that any assumed shape unintentionally introduces a constraint on the system (adding additional stiffness to the system) and so the estimated frequency is always greater than or equal to the exact value. Rayleigh's principle may be applied to slabs in the same manner as for beams but, due to more complex boundary conditions and mode shapes, it is not often used in practice. For higher frequencies, the Rayleigh approach can be extended by representing the total motion as the sum of several assumed mode shapes; this is known as the Rayleigh-Ritz method.

Stodola method

This is an iterative static analysis method which provides an estimate of the fundamental frequency by an approximation of the dynamic mode shape. The estimated mode shape is first multiplied by the mass to derive a value of force proportional to the inertial force. This imaginary inertial force is then applied to the system and the resulting deflection, once normalised, is an updated better approximation of the mode shape. The procedure is continued until the mode shape no longer changes significantly between iterations. Convergence is normally achieved after two or three iterations. Hence, the square of the angular frequency is estimated by dividing the previous mode shape by the resulting displacement [Clough and Penzien (1993), Timoshenko et al. (1974)].

Dunkerly's principle

This method gives the approximate value of the fundamental frequency of a system in terms of the natural frequencies of the component parts. For an idealised floor system with the slab fundamental frequency, f_{01}, floor beam frequency, f_{02}, and main beam frequency, f_{03}, the fundamental system frequency, f_0, is obtained from:[Allen (1974)]

$$\frac{1}{f_0^2} = \frac{1}{f_{01}^2} + \frac{1}{f_{02}^2} + \frac{1}{f_{03}^2} \tag{2.13}$$

This method is more relevant to composite steel-concrete floors, which have separate components. For post-tensioned floors, it may be used to consider the main slab and its support beams.

Continuous spanning slabs

The simplest case of a continuous spanning system is a two-span beam. With equal spans, it is possible to consider only a single span since, in the fundamental mode, adjacent spans act in opposite directions due to inertial forces (figure 2.12). Making the spans unequal, would have

a stiffening effect, thus increasing the natural frequency. For multiple span beams, graphs are available to aid the calculation of natural frequencies [SCI (1989)].

CSA (1989) suggests the use of the simple beam formula to calculate natural frequencies of continuous beams. It suggests obtaining a dynamically equivalent simply supported beam from the span and restraint conditions of a continuous one. This requires an assumption of the mode shape, which in some cases may be very crude due to uncertainties in boundary conditions. Hence, care should be taken in decreasing the span length to obtain an *equivalent simply supported span*, as erroneous estimates of frequency may result [Caverson et al. (1994)].

2.5.3 Practical methods of frequency estimation

The theory introduced above can be used to estimate the frequencies of real floors in practice. However, the determination of the exact floor vibration natural frequencies is by no means straightforward, if all variables are considered. The complexity of the exact computation has prompted investigators to propose simplified approaches, three of which are discussed below.

Equivalent beam method (EBM)

This is the most commonly used method of predicting the fundamental natural frequency of a floor, as presented by Murray (1975) for composite steel-concrete slabs. The slab is approximated as a beam with transformed width and second moment of area, (figure 2.14), and the fundamental natural frequency is given as:

$$f_0 = K\sqrt{\frac{EI_t}{wL^4}} \tag{2.14}$$

where values of K depend on boundary conditions and are given as 1.57 for simply supported, 2.45 for fixed/simply supported, 3.56 for fixed/fixed, and 0.56 for a cantilever beam. For a simply supported beam, this formula is identical to the solution derived in equation 2.8. For the purposes

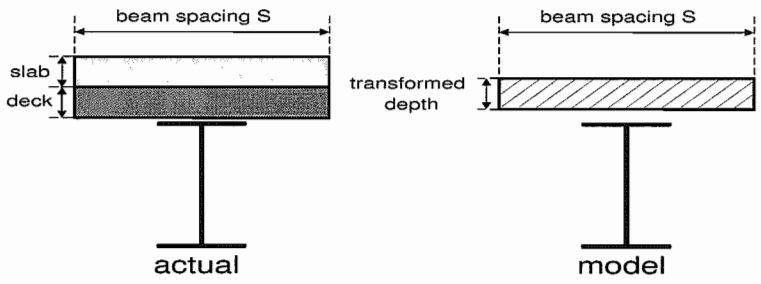

Figure 2.14: Murray(1975) transformed beam

of calculation of second moment of area, SCI (1989) suggests the effective width of slab to be the smaller of either $L/4$ or the beam spacing. Allen and Murray (1993) suggested the smaller of $0.4L$ or the beam spacing.

The EBM is seen by a number of researchers to give acceptable estimates of floor fundamental frequency [Chang (1973), Allen (1974), Murray (1975), Allen et al. (1979), Pernica and Allen (1982), SCI (1989)]. However, caution must be exercised in the application of this formula to two-way spanning floors. The limitations of this method are: (1) higher modes of vibration are not considered, (2) the state of the concrete cross-section (degree of cracking and modulus of elasticity) are uncertain, (3) for slabs with deep joists or trusses, expressing the natural frequency in terms of second moment of area can lead to substantial errors, mainly due to shear deformation effects of the joists [Allen et al. (1985)], and (4) its application to continuous slab systems and the determination of the dynamically equivalent simply supported span [CSA (1989)] are questionable. In a comparison carried out between predicted and experimental results, Williams and Waldron (1994) found that for post-tensioned concrete slabs, the EBM underestimated the real frequencies by between 17% and 54%. Hence, this method is unreliable for two-way spanning slabs.

Static deflection method

This approach uses the classical mass-spring system for calculating natural frequencies, as given in equation 2.6 in terms of static deflection [Allen et al. (1985), SCI (1989), Allen (1990b), Allen and Murray (1993), AISC (1997)]. Furthermore, for a composite one-way slab with uniform load, Dunkerly's principle can be used to obtain the system static deflection: [Allen (1990b)]

$$\Delta_s = \frac{\Delta_b + \Delta_g}{\lambda} + \Delta_c \tag{2.15}$$

where Δ_s is the total static deflection and Δ_b, Δ_c and Δ_g denote static deflections of beams, columns and girders respectively. λ is the transformation factor from real systems to equivalent SDOF systems. It takes the values of 1.3 for a simply supported beam and 1.5 for two-way slabs and fixed cantilevers. This method will give lower frequencies than the EBM, since it allows for shear and column deflections in addition to bending estimates. Since the EBM already underestimates values of frequency [Williams and Waldron (1994)], the effectiveness of the method on concrete floors is questionable. The main limitation of this method is that it requires the calculation of static deflections, which are difficult to carry out particularly for two-way slabs.

Concrete Society method

The Concrete Society (1994) proposed a calculation procedure for two-way slabs, in which vibration is assumed to occur in two independent orthogonal modes, in the two span directions. This method makes use of the EBM, but introduces modification factors to account for the increased stiffness of a two-way member. Account is also taken of the type of slab, aspect ratio, and boundary conditions. The method yields two natural frequencies, corresponding to independent modes in the two span directions. The formulae and procedures are given below in the x-direction for solid or waffle slabs only. The characteristics of the y-direction mode can be determined by interchanging the x and y subscripts in these equations.

Firstly, the effective aspect ratio of a slab panel is defined as:

$$\lambda_x = \frac{n_x l_x}{l_y} \left(\frac{EI_y}{EI_x} \right)^{\frac{1}{4}} \tag{2.16}$$

where n_x is the number of bays in the x-direction and l_x, l_y are bay spans in the x and y directions. This is used to calculate a modification factor k_x:

$$k_x = 1 + \frac{1}{\lambda_x^2} \tag{2.17}$$

For slabs with perimeter beams, the natural frequency is then:

$$f'_x = \frac{k_x \pi}{2} \sqrt{\frac{EI_y}{W l_y^4}} \tag{2.18}$$

For slabs without perimeter beams, an intermediate frequency is first calculated, which is used to modify equation 2.18:

$$f_b = \frac{\frac{\pi}{2} \sqrt{\frac{EI_x}{W l_x^4}}}{\sqrt{1 + \frac{EI_x l_y^4}{EI_y l_x^4}}} \tag{2.19}$$

The natural frequency is then:

$$f_x = f'_x - (f'_x - f_b) \left[\frac{1}{2n_x} + \frac{1}{2n_y} \right] \tag{2.20}$$

Similar calculations for the other slab types (e.g. ribbed slabs) are also given. As can be seen, this method is highly complex involving many parameters and equations. Furthermore, the mode in the x-direction is seen to depend on y-direction bending properties (equation 2.18), the reasons for which are not explained. Williams and Waldron (1994) found little agreement between their field results and predictions of natural frequency using this method. It was seen to under-predict the actual frequencies in all their cases, sometimes by as much as 77%.

2.6 Damping

Damping is a mechanism by which vibrational energy is gradually converted to heat or sound, resulting in a slow decrease of the response of a system. It can arise from almost any structural or non-structural element, and thus, is very hard to predict theoretically. The causes of damping are also difficult to determine, hence it is modelled as one or more of the following types:

Viscous damping: This is a common form of damping, which depends on the material properties of the structure. Here, the damping force is proportional to the velocity of the vibrating body, and always opposes the motion, resulting in an exponential decay of oscillations.

Coulumb, or friction, damping: Here, the damping force is constant in magnitude but opposite in direction to the motion of the vibrating body. It is caused by friction between rubbing surfaces that are either dry or have insufficient lubrication. This cause of damping is independent of frequency and the resulting decay of oscillations is linear. In concrete, Coulomb damping at the cracks and joints is one of the major causes of energy dissipation.

Material, or hysteretic, damping: When materials are deformed, energy is absorbed and dissipated by the material. The effect is due to friction between internal planes, which slip or slide as the deformations take place. When a body having hysteretic damping is subjected to vibration, the stress-strain diagram shows a hysteresis loop. The area of this loop denotes the energy lost per unit volume of the body, per cycle, due to damping. In concrete, hysteresis damping is most likely to occur at the cracks.

Radiation damping: This is the amount of energy that radiates outwards from the floor into the surrounding structural components, such as columns.

2.6.1 General definitions

In most mathematical models, the combined damping effect is assumed to be in the form of *equivalent viscous damping*, as this involves linear equations, which are relatively easy to solve. A viscous damper can be constructed using two parallel plates separated by a distance, h, with a fluid of viscosity, μ, between the plates (see figure 2.15). If the top plate moves with a velocity v, there is assumed to be a linear variation of the velocities of intermediate layers between 0 and v, the velocity gradient being: $\frac{du}{dy} = \frac{v}{h}$. The shear or resisting force, F, developed at the bottom surface of the moving plate is:

$$F = \tau A = \frac{\mu A v}{h} = cv \tag{2.21}$$

where τ is shear stress and c is called the *viscous damping constant* given by:

$$c = \frac{\mu A}{h} \tag{2.22}$$

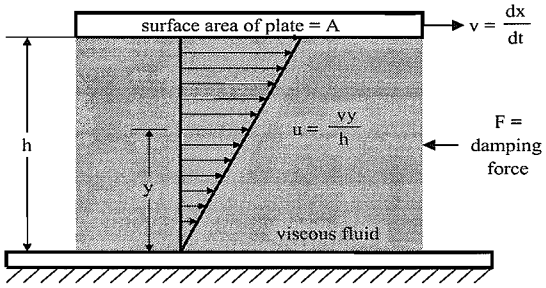

Figure 2.15: Example of viscous damping mechanism

In theoretical analyses, a damper is assumed to have neither mass nor elasticity and damping force exists only if there is relative velocity between the two ends of the damper. It is illustrated in figure 2.16(a) by a dashpot, which is usually in parallel to a spring representing the stiffness of the material. This is known as the Kelvin-Voigt model [Bert (1973)].

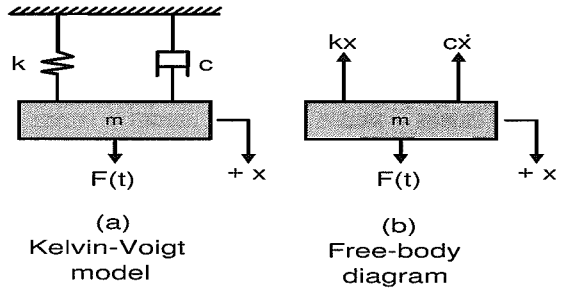

Figure 2.16: SDOF Kelvin-Voigt spring-mass-damper model

The application of Newton's second law to figure 2.16(b) yields the equation of motion:

$$m\ddot{x} + c\dot{x} + kx = 0 \tag{2.23}$$

By solving in the usual way, the roots of the characteristic equation are expressed as:

$$-\frac{c}{2m} \pm \sqrt{\left(\frac{c}{2m}\right)^2 - \frac{k}{m}} \tag{2.24}$$

The *critical damping*, c_c, is defined as the value of the damping constant, c, for which the radical in equation 2.24 becomes zero, hence making the vibration non-oscillatory:

$$c_c = 2m\sqrt{\frac{k}{m}} = 2m\omega_n \tag{2.25}$$

For any damped system, the *damping ratio*, ζ, is defined as:

$$\zeta = \frac{c}{c_c} \tag{2.26}$$

This is the conventional way of expressing damping in civil engineering structures.

2.6.2 Methods of structural damping measurement

The determination of the damping capacity of a system usually depends on the method of measurement employed. It can be derived from: (a) energy dissipation, (b) decay of free vibrations, (c) reduction of resonant response, or (d) phase difference between force and displacement [Ungar (1963)]. Here, two common methods are described in the time and frequency domains.

Logarithmic decrement method

The logarithmic decrement represents the rate at which the amplitude of free damped vibration decreases. It is defined as the natural logarithm of the ratio of any two successive amplitudes. In figure 2.17, if x_1 and x_2 denote the amplitudes corresponding to times t_1 and t_2, measured one cycle apart, the ratio of x_1 to x_2 is:

$$\frac{x_1}{x_2} = \frac{e^{-\zeta\omega_n t_1}}{e^{-\zeta\omega_n(t_1+T)}} = e^{\zeta\omega_n T} \tag{2.27}$$

The logarithmic decrement is then:

$$\delta = \ln\frac{x_1}{x_2} = \zeta\omega_n T = \frac{2\pi\zeta}{\sqrt{1-\zeta^2}} \tag{2.28}$$

Similarly, if the displacements are measured over any number of complete cycles, r:

$$\delta = \frac{1}{r}\ln\left(\frac{x_1}{x_{r+1}}\right) \tag{2.29}$$

From equation 2.28, δ can be related to the damping ratio, ζ, thus:

$$\zeta = \frac{\delta}{\sqrt{(2\pi)^2+\delta^2}} \tag{2.30}$$

Hence, the damping in a system can be measured experimentally from the time-domain data of free damped oscillation. One draw-back is that ζ is often amplitude dependent, thus from different parts of the decay curve different damping quantities result [Ellis and Ji (1996)]. For purely viscous damping, the dotted envelope line in figure 2.17 is an exponential decay, and for pure friction damping it is a straight line decay. For real structures, the envelope line generally lies inbetween these two cases [Bachmann et al. (1995)].

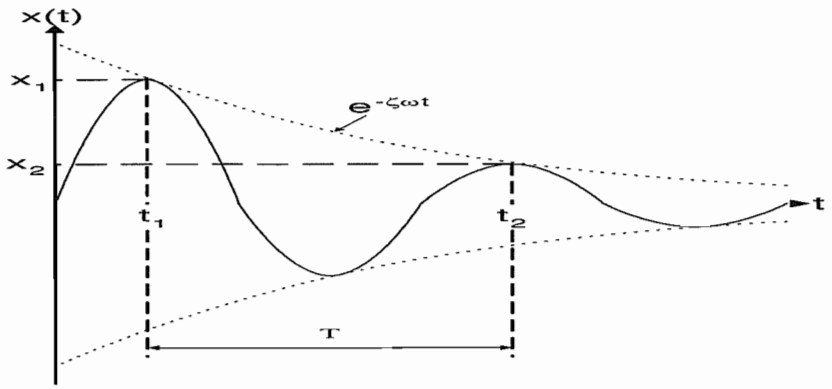

Figure 2.17: Time-domain logarithmic decay method

Halfpower bandwidth method

This method uses the frequency-domain response curve to determine damping from the amplification factor at a resonant mode (see figure 2.18). For a SDOF system, the dynamic amplification factor (DAF) is expressed as:

$$DAF = \frac{1}{\left[\left(1-\left(\frac{\omega}{\omega_n}\right)^2\right)^2 + \left(2\zeta\frac{\omega}{\omega_n}\right)^2\right]^{\frac{1}{2}}} \tag{2.31}$$

where ω_n is the natural frequency of the system and ω is the forcing frequency. At resonance, $\omega = \omega_n$ and equation 2.31 reduces to:

$$Q = \frac{1}{2\zeta} \tag{2.32}$$

where Q is the amplitude at resonance. The points R_1 and R_2, where the amplification falls to $\frac{Q}{\sqrt{2}}$, are called *half-power* points and the difference between R_2 and R_1 is called the *bandwidth* of the system. This can be found by equating the dynamic amplification of the system to $\frac{Q}{\sqrt{2}}$:

$$\frac{Q}{\sqrt{2}} = \frac{1}{\left[\left(1-\left(\frac{\omega}{\omega_n}\right)^2\right)^2 + \left(2\zeta\frac{\omega}{\omega_n}\right)^2\right]^{\frac{1}{2}}} \tag{2.33}$$

For small ζ, the solution of equation 2.33 is:

$$\omega_{1,2} = \omega_n\sqrt{1 \pm 2\zeta} \quad \approx \quad \omega_n\left(1 \pm \zeta\right) \tag{2.34}$$

Hence, if ω_1 is the value of frequency at R_1 and ω_2 is the frequency at R_2, $\omega_2 - \omega_1 \simeq 2\zeta\omega_n$, and the damping ratio for the system is given by:

$$\zeta = \frac{\omega_2 - \omega_1}{2\omega_n} \tag{2.35}$$

For complex structures with closely spaced modes, the resonance curves can be difficult to evaluate

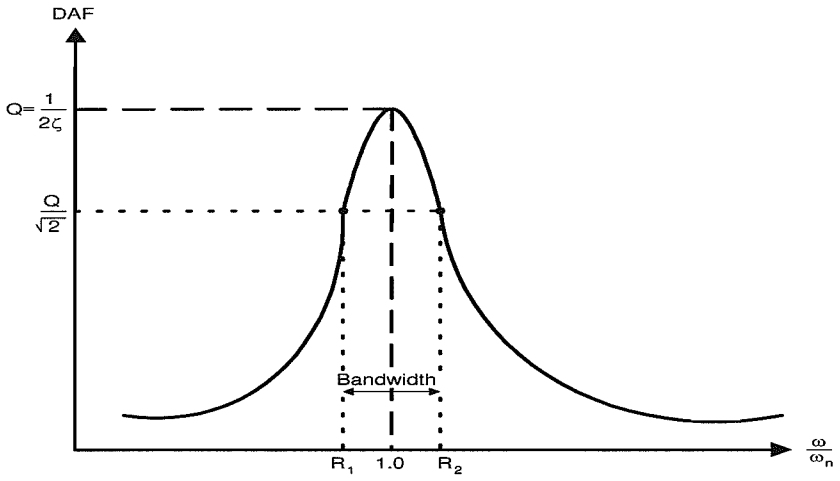

Figure 2.18: Frequency-domain halfpower bandwidth method

and curve-fitting techniques may be required to separate the individual peaks. Hence, the application of this method to complex systems can become cumbersome. Moreover, non-linear behaviour of a structure may lead to disturbances at the resonant peak, with the result that for a certain value of $\frac{\omega}{\omega_n}$, two (or three) different amplitudes may occur. This makes it difficult to evaluate the resonance curve. Hence, with this method, measuring errors can greatly affect the determination of the damping quantity.

2.6.3 Damping mechanisms in concrete

Material damping in concrete elements is mainly due to cracking and depends strongly on the stress level. Figure 2.19 shows the equivalent damping ratio of a bending element [Bachmann et al. (1995)]. For low stress, corresponding to the uncracked state, a relatively low damping ratio (ζ <1%) exists. As cracks form, the damping ratio increases. In the cracked state, but still with relatively low stress, the damping ratio is relatively high, perhaps two or three times the value of the initial uncracked state. With a further increase in stress, the damping ratio decreases rapidly and may reach a value smaller than that of the initial uncracked state. This damping behaviour may be explained as follows:

- in the uncracked state, nearly pure viscous damping occurs in the concrete
- in the cracked state, two kinds of damping occur
  - nearly pure viscous damping in concrete uncracked compression zone
  - nearly pure friction damping, due to friction between concrete and reinforcing steel, in the cracked tension zone

The actual behaviour of the concrete can be represented by its equivalent viscous damping ratio, ζ_{eq}, incorporating both means of energy dissipation:

$$\zeta_{eq} = \frac{1}{4\pi} \frac{\text{energy dissipation per cycle}}{\text{maximum potential energy}} \tag{2.36}$$

Note that the maximum potential energy in a structure is proportional to the square of the stress intensity, as is the energy dissipation per cycle due to viscous damping [Bachmann et al. (1995)]. Hence, at a constant depth of the compression zone, a viscous damping component of ζ results, which is independent of the stress intensity (see figure 2.19). On the other hand, the energy dissipation per cycle due to friction is linearly proportional to the stress intensity and a friction damping component of ζ results, which decreases hyperbolically with increasing stress intensity (figure 2.19).

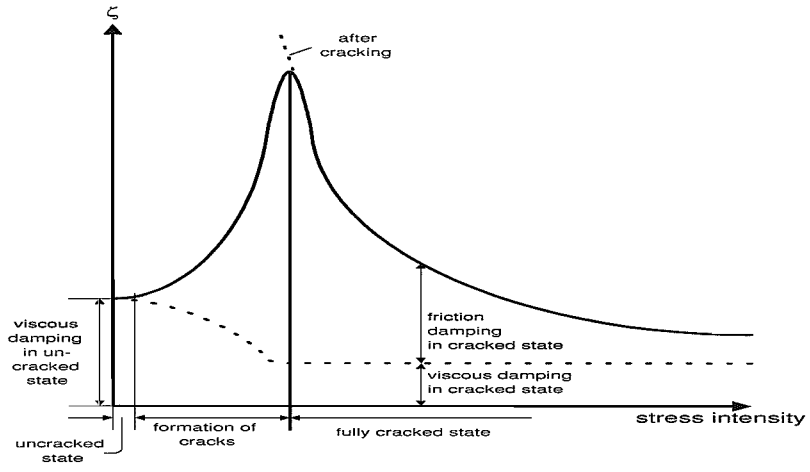

Figure 2.19: Damping mechanisms in concrete with increasing stress intensity

Overall damping of a floor structure

Depending on the location of energy dissipation, the total overall damping of a floor structure is the sum of the contributions from the bare structure, non-structural elements, and energy radiation to surrounding structural components. Contributions by non-structural elements depend on their number, type, and relative dimensions. This contribution may be greater than the equivalent damping ratio of the bare structure alone. This explains why different structures or structural types, made of the same materials, may have very different overall damping ratios. The energy radiation to the soil, through walls or columns by travelling waves, may be significant but is difficult to quantify. The overall effect of all the above contributions to the damping of a floor can not yet

be stated with confidence. The estimation of the overall equivalent viscous damping ratio of a structure is largely based on the judgement and experience of the engineer.

2.6.4 Review of measurement practice and results

The first rigorous investigation into the damping characteristics of concrete was carried out by Penzien (1964), who tested a total of 20 prestressed concrete beams. He found that most of the equivalent viscous damping factors ranged from 0.5% to 7%, depending on the degree of cracking permitted in each test due to prestressing.

Lenzen (1966) tested actual concrete floors and found that floors for which vibrations were barely or not at all perceptible had damping exceeding 5%, and the vibrations were definitely perceptible in floors with damping less than 3%. The inclusion of partitioning and mechanical services increased damping to well above 6% for most floors.

Murray (1975) suggested values of floor damping ratios based on slab thickness. These are similar to Allen (1974), Allen and Rainer (1976) and CSA (1989) recommendations. Murray's suggested values are: bare floor, ζ=1-3% (depending on slab thickness and concrete mix design); ceilings, ζ=1-3% (lower limit for hung ceiling and upper limit for ceilings attached to beams); ductwork and mechanical equipment, ζ=1-10% (depending on amount); and partitions, ζ=10-20% (if attached to the floor system). Murray also recommended that for floor systems with damping ratios more than 8-10%, there would be no need for vibration analysis. AISC (1997) recommends that these values be halved since they are derived using heeldrop tests, which include transmission of energy to other structural components, whereas modal damping excludes vibration transmission.

Farah et al. (1977) commented on the merits of using constrained viscoelastic materials to damp floor vibrations. This technique would be most useful in composite floors, where the viscoelastic layer would be applied to the bottom flange of the supporting beams and can be constrained using metal plates. Nelson (1968) reported three such applications with notable increases in damping capacity. Moiseev (1991) suggested using layers of concrete treated with viscoelastic admixtures to reduce vibrational response of floors. He described results of tests on two floors in which the addition of such damping layers reduced peak vibration velocities by as much as 60%, compared with predicted values of floors without the layers. A 20% increase was observed in the actual damping ratios of the floors and Moiseev commented that care should be taken with the use of the admixures due to possible changes in the concrete properties.

Caverson et al. (1994) presented field test results, in which they found the mean damping ratios for prestressed floors and reinforced concrete floors to be similar at around 2.2%, and to be higher than the value for their composite floor at 1%. They also found that non-structural elements, such as false ceilings and false floors, significantly increased the damping ratios of floors to around 2.7-4.7%. These results agree well with Murray's suggested values. Pernica (1987) tested a slab before and after installation of non-structural components and found a marked increase in damping.

In summary, the overall value of damping inherent in a structure is dependent on many factors, such as the structure's geometry and non-structural components present, and is hence very difficult to estimate. Even now, engineers and designers select values of damping based on previous results of similar structures, or on their own past experience. It is hence commonly accepted that further research is required in this field to achieve better estimates of structural damping capacity.

2.6.5 Tuned mass dampers (TMDs)

A tuned mass damper (or vibration absorber) is a vibratory subsystem attached to a larger primary vibration system. The normal function of the absorber is to reduce resonant oscillations of the primary system. Accurate tuning of the frequency of the absorber results in induced inertia forces of the absorber mass, which counteract the forces applied to the primary system. While the vibration amplitudes of the primary system can be suppressed to a large extent, large displacement amplitudes must be accepted in the absorber system.

In most cases, vibration at one natural frequency of the primary system is troublesome and requires attenuation. When tuned to the troublesome frequency, an absorber can substantially reduce the maximum displacement amplitude of the primary system. The absorber hardly affects the response of the primary system away from the optimum absorber frequency.

Practical applications

The application of TMDs can be considered whenever critical dynamic forcing cannot be avoided and the structure cannot be stiffened economically. TMDs are only effective in certain types of structures, such as buildings and bridges, which demonstrate high displacement values. The first use of TMDs can be dated back to 1911 when they were used to reduce the rolling motion of ships, and also for the reduction in ship hull vibrations [Setareh and Hanson (1992a)]. For civil engineering applications, McNamara (1977) investigated the effectiveness of TMDs in buildings and found a

significant increase in their damping ratios. Bachmann (1992b) installed TMDs on footbridges and found that their inclusion reduced acceleration amplitudes by a factor as high as 20.

Until recently, the application of TMDs on floors was very rarely considered and mainly confined to laboratory experiments [Lenzen (1966)]. This was because most floors exhibit several closely spaced natural frequencies requiring an array of TMDs, making the operation uneconomical. Problems may also arise with their maintenance and re-tuning [Allen (1990a)], although recently adaptive TMDs have been developed with self-tuning capabilities [Rade and Steffen (1999)]. Some successful applications of TMDs to floors have been reported. Webster and Vaicaitis (1992) installed a TMD system in a composite floor and managed to reduce floor vibrations by as much as 60%. Setareh and Hanson (1992b) applied absorbers to a cantilever concert hall balcony, reducing vibration amplitudes by 78%. However, in both of these cases, the construction was of high displacement and low damping, which makes the use of TMDs more effective. Their use on normal simply supported two-way floors, in which the displacements are much smaller, will require more research.

2.6.6 Human-structure interaction

In this section, the interaction between a floor and its occupants is discussed as far as the response and energy absorption of a human body is concerned. This may be significant if the mass of the people is reasonably large in comparison with the mass of the structure. In this case, it is possible that the interaction between the people and the structure could effectively change the system characteristics. Existing methods of considering people in structural vibrations are varied and sometimes inconsistent. Some design codes treat human action as simply a load [BS5400 (1978), CSA (1989)], whereas studies of the human body suggest that it should be modelled as a spring-mass-damper system [Ellis and Ji (1997), Foschi et al. (1995), Folz and Foschi (1991)].

A simple model of human-structure interaction can be obtained by treating each as a SDOF system, so that they combine to give a 2DOF system. This is similar to the basic model of a structure-TMD setup, with some important differences:

- The mass ratio between humans and a structure is likely to be much higher than that of a TMD. This may affect the validity of the reduction of the structure to a SDOF system, which is based on the structure without the secondary system.
- For a TMD setup, the fundamental frequency of the absorber is a design variable that is tuned. The frequency of the human body, however, is constant for a given person and posture, typically between 4-6Hz when sitting and 8-10Hz when standing [Fairley and Griffin (1989)].

- The damping ratio of a TMD system is also a design variable, whereas that of a human body is a constant and can be as large as 47.5% at its sitting position [Ji and Ellis (1994b)].
- The human body is not always present on the structure and its effect as an energy absorber may be completely lost when it changes from a stationary state to a moving state.

A similar, but slightly more complex, representation of the human body is proposed by ISO2631/1 (1985), where the body is modelled as a 2DOF system with prescribed parameters. The two natural frequencies of this model are 5.03Hz and 12.49Hz. Folz and Foschi (1991) utilised this model in a numerical study supported by experiments on a composite floor and found good agreement. Foschi et al. (1995) stipulated that the second frequency does not have a significant influence on the response and so a SDOF system would suffice as a model. Other, more elaborate, representations of the human body include the 15DOF model introduced by Nigam and Malik (1987), and a continuous model of the body in the standing position proposed by Ji (1995).

Practical results

Currently, the subject of human-structure interaction is poorly covered in the literature and only a few notable findings can be recorded. Most investigations have involved structures such as grandstands, where the number of people present is high. Ellis et al. (1994) tested a cantilevered grandstand when empty and when occupied during a sports event. They found that with the crowd, an additional frequency was observed that did not exist when empty. They also noticed a significant increase of damping when people were involved. They concluded that the crowd can be modelled as a spring-mass-damper system, which interacts with the structure to form a 2DOF system, hence the appearance of two frequencies and increased damping. Pernica (1983) also observed increased damping with crowd involvement.

2.7 Floor accelerations

In general, there are two approaches to the design of structures to accomodate dynamic occupant loads. One relies on ensuring the fundamental natural frequency of the structural system is sufficiently high that resonances produced by occupant movements are avoided, the other provides a method for calculating structural response to dynamic loads so that a structural design can be checked. The approaches therefore are to *avoid* or *design* for the problem. In the following section, the second of these approaches is considered.

The response of a floor to occupant movements depends on the mass of the floor, its dynamic characteristics, such as natural frequency and damping, and on the nature of the input loading. The most common parameter used in the analysis of floor dynamic response is the value of the vertical acceleration of the slab caused by a given loading function. Most acceptability criteria for human perception of vibration use this parameter (see section 2.2.2). Here, methods of calculating acceleration amplitude are first discussed as a result of simplified loading functions. The various design guidelines in use, for limiting floor response, are described in section 2.7.2.

2.7.1 Estimation methods

To enable accurate estimation of the response of a floor, it is first necessary to consider the applied loading. Due to the complexity of analysing the response to a typical walking force, most design methods use a simplified empirical approach. The heeldrop test was developed as a result of this need and is used in most of the methods for estimating initial acceleration.

Allen and Rainer (1976) and Pernica and Allen (1982) suggested that for floors longer than 7.6m, with frequencies less than 10Hz, initial acceleration amplitude from a heeldrop can be estimated assuming it is suddenly applied to a simple spring-mass system giving:

$$A_0 = \frac{2\pi f_0 P(0.9)}{M} \tag{2.37}$$

where M is the equivalent mass of the oscillator, P is the impulse force due to a heeldrop (70Ns), and the value of 0.9 accounts for the loss of amplitude due to damping before reaching the first peak. SCI (1989) ignores this factor thus arriving at a marginally higher prediction.

CSA (1989) gives a formula for the peak acceleration amplitude of composite floors, assuming heeldrop loading and that a fixed width of floor, b, participates in the response. Hence:

$$A_0 = \frac{60 f_0}{w_t b L} \tag{2.38}$$

where w_t is the weight of the floor plus contents. This method requires the estimation of natural frequency, which is calculated by EBM (section 2.5.3). Williams and Waldron (1994) found very poor agreement between acceptability ratings of this approach with experimentally measured parameters on prestressed concrete floors.

For rhythmic dance-type loads, in a departure from assuming the heeldrop, Ji and Ellis (1994a) used equation 2.3 (page 18) as the loading function. They hence presented an analytical solution for the forced vibration of simply supported floors, using plate theory, and considered several modes of

vibration. For this method, an assumption of the fundamental mode shape of the floor is required and the steady-state acceleration response, A_{st}, is given as:

$$A_{st} = B\frac{G_d}{W}(DLF) \tag{2.39}$$

where W is the mass of the empty floor per unit area, and B is defined as the structural factor depending on type of structure and boundary conditions. DLF is the acceleration dynamic magnification factor, for which the peak value of the nth Fourier component is defined as:

$$(DLF)_{peak} = \frac{\alpha_n n^2 \left(\frac{f_p}{f}\right)^2}{\sqrt{\left(1 - n^2\left(\frac{f_p}{f}\right)^2\right)^2 + \left(2n\zeta\frac{f_p}{f}\right)^2}} \tag{2.40}$$

where α_n is the nth Fourier coefficient of loading. In a verification of this method, Ellis and Ji (1994) found good agreement with experimental and numerical results. This solution is also recommended in BRE 426 (1997) and corresponds with ISO10137 (1992) and annex A of BS6399 (1996).

Note that the above methods necessitate the prediction of floor dynamic characteristics, which can be inaccurate. Murray (1975) observed that the calculated floor response is highly sensitive to the predicted natural frequency and to the amount of the floor which participates in response.

2.7.2 Design guidelines

Design methods have been developed to combine all relevant parameters of floor vibration, such as human perception, natural frequency, and dynamic loading, to limit floor vibration responses. This section presents four such guidelines.

CSA (1989) Appendix G

The CSA guideline for composite floors requires calculation of fundamental frequency by the EBM (equation 2.14), and estimation of the peak acceleration due to a heeldrop, using equation 2.38. The acceptibility of the floor is then checked using the perceptibility diagram of figure 2.4. The drawbacks of this method include the use of heeldrop to predict walking vibration annoyance, and the estimations of parameters that can be inaccurate. In assessing its reliability for concrete floors, Williams and Waldron (1994) found very poor agreement. Hence, as it stands, this approach is unsuitable for concrete floors, unless the estimation of parameters is clarified for use with such floors.

SCI (1989) Guide

The SCI guide is based on the actual calculation of human response by introducing a new parameter called *the response factor*. Firstly, floors are separated into two categories: low frequency $\leq$ 7Hz $\leq$ high frequency. Then, the response factors of the floors are estimated. For low frequency floors, resonance with the walking force ($\approx$2Hz) is considered, whereas for high frequency floors, the response factor is based on the impulse response to a heel-impact, assuming no resonance effects. Empirical formulae are given to calculate the response factors that should not exceed tabulated limits. These limits account for three cases of general, special and busy office environments.

Concrete Society (1994) handbook

The Concrete Society present an elaborate method for calculating a similar response factor to the SCI (1989) guide. For concrete floors, the calculation of response factor, R, follows directly from the prediction of the natural frequencies by their method (see section 2.5.3). Firstly, two response factor coefficients, N_x and C_x, are calculated. These equations apply to solid or waffle slabs only.

$$N_x = 1 + (0.5 + 0.1 \ln \zeta)\, \lambda_x \tag{2.41}$$

$$\begin{aligned}
f_x \leq 3Hz \qquad & C_x = 224.8/(f_x \zeta) \\
3Hz \leq f_x \leq 4Hz \qquad & C_x = 27.2/\zeta \\
4Hz \leq f_x \leq 5Hz \qquad & C_x = (83.2 - 14 f_x)/\zeta \\
5Hz \leq f_x \leq 20Hz \qquad & C_x = \frac{0.88\,(20 - f_x)}{\zeta} + 2\,(f_x - 5) \\
20Hz \leq f_x \qquad & C_x = 30
\end{aligned} \tag{2.42}$$

The response factor in the x-direction is then given by:

$$R_x = \frac{C_x N_x}{W n_x n_y l_x l_y} \tag{2.43}$$

Application of equations 2.41 to 2.43 is repeated for the slab spanning in the y-direction, simply replacing all the x subscripts by y; the overall response factor is then $R = R_x + R_y$. For an acceptable floor, R must not exceed 4 in a sensitive environment, 8 in a general environment and 12 in a busy environment. Williams and Waldron (1994) found generally good agreement of this method with their experimental results, although in some cases, the calculated response factor was excessively conservative.

AISC (1997) design guide

This is the most recent design guide for composite floors. The approach it recommends was developed by Allen and Murray (1993) and is based on the ISO2631/2 (1989) and BS6472 (1984) acceptability scales (figure 2.5). The excitation force is taken as the first harmonic of pedestrian activity (equation 2.2), and the fundamental frequency of the composite floor is derived by the static deflection method (section 2.5.3), where Dunkerly's principle is used to account for the deflections of the beam and the girder (equation 2.15). The guideline then differentiates between walking and rhythmic excitations. For walking excitation, the response is given in terms of induced acceleration:

$$A_{rms} = \frac{gP_0 e^{-0.35 f_0}}{\sqrt{2}\zeta W_e} \tag{2.44}$$

where P_0 is a constant force representing the excitation (given as 0.29kN for floors) and W_e is the effective weight of the floor supported by the beam, girder, or combined panel (calculated from the effective width). The value of A_{rms} is then checked and should be less than the relevant ISO/BSI/ANSI curve (figure 2.5), or the limits of $0.5\%g$ for offices or $1.5\%g$ for shopping malls. Values of damping are given as ζ=2-5% for offices and 2% for shopping malls. Furthermore, the guide suggests that for fundamental frequencies greater than 9Hz, the minimum stiffness criterion of 1kN/mm should be used in addition to the walking excitation criterion. Murray (1999) comments that in using this guideline, careful estimates of the actual live load on the floor during normal occupany, and of the damping ratio, are required for a successful design.

The AISC criterion of equation 2.44 is a modified version of the one developed by Allen and Murray (1993). They started by defining an acceleration limit and used it to determine a minimum acceptable floor fundamental frequency:

$$f_0 \geq 2.86 \ln\left[\frac{K}{\zeta W_t}\right] \tag{2.45}$$

Here, W_t is the total weight supported by one beam and K is a force constant. Comparing with equation 2.44, $K = \frac{gP_0}{\sqrt{2}A_{rms}}$, so that it accounts for both the exciting force and the acceleration limit. K is specified as 58kN for offices and 20kN for shopping malls. This relaxation for more active occupancies is similar to increasing the acceleration limit by a factor of three, as recommended by Pernica and Allen (1982), see section 2.2.2. In comparison with other criteria, generally good agreement in the frequency range of around 5-8Hz was found, beyond which the CSA and SCI methods become more conservative.

For rhythmic activities, AISC (1997) assumes the structure to have only one mode of vibration and derives the peak acceleration of the floor as:

$$A_{rms} = \frac{Jg\alpha_i \frac{w_p}{w_t}}{\sqrt{2}\sqrt{\left[\left(\frac{f_0}{f}\right)^2 - 1\right]^2 + \left[\frac{2\zeta f_0}{f}\right]^2}} \tag{2.46}$$

where α_i is the dynamic coefficient of the forcing function, f is the forcing frequency, w_p is the effective weight of participants per unit area, w_t is the effective weight of floor and occupants per unit area, and J is a constant depending on activity (taken as 1.3 for dancing, 1.7 for sport events, and 2.0 for aerobics). The resulting acceleration should again be smaller than the relevant ISO/BSI/ANSI curve or the limits of 0.4-0.7%g for offices and 1.5-2.5%g for dining halls.

2.8 Remedial measures for problematic floors

While research is being conducted to introduce design codes for serviceability vibrations, floors are still being built, which have vibration problems. Remedial measures are needed for controlling undesirable vibrations in existing structues. These generally fall into four categories.

Frequency Tuning

Here, the fundamental frequency of the structure is measured and the structure is stiffened in such a way that the possibility of resonance is eliminated. For a satisfactory design, the ratio between the floor fundamental frequency and the disturbing frequency should be outside the range 0.5 to 1.5 [Fowler and Karabinis (1979)]. It is highly recommended that this ratio should be on the high side of the range so that the floor responds to the applied dynamic force as though it was a static force. The stiffening process can range from adding extra columns to beam stiffening. Guidelines have also been presented giving limits on the minimum value of natural frequency for satisfactory vibration design of floors, table 2.5. For synchronised dance-type loads, BS6399 (1996) recommends a minimum fundamental frequency of 8.4Hz for vertical vibrations. Note that other important factors, such as floor span-depth ratios and damping, are not considered in these criteria.

Table 2.5: Bachmann (1992a) recommended natural frequencies of structures

Structure type	Construction type			
	reinforced concrete	prestressed concrete	composite steel-concrete	steel
gymnasiums and sports halls	> 7.5	> 8.0	> 8.5	> 9.0
concert halls, theatres, and spectator galleries with fixed seating. Classical or soft pop music concerts	> 3.4	> 3.4	> 3.4	> 3.4
concert halls, theatres, and spectator galleries with fixed seating. Hard pop music concerts	> 6.5	> 6.5	> 6.5	> 6.5
dance halls and concert halls without fixed seating	> 6.5	> 7.0	> 7.5	> 8.0
note: for footbridges avoid 1.6-2.4Hz (with low damping also 3.5-4.5Hz)				

Limiting vibration amplitudes

Here, the vibration amplitudes are measured and the structures are upgraded by adding extra stiffness, such as columns, so as to ensure that certain allowable values are not exceeded. In comparison to frequency tuning, this method is theoretically more exact as it also requires the calculation of a forced vibration response and the damping properties of the structure. This would lead to uncertainties as there are no accurate methods of predicting various structural dynamic parameters.

Increasing damping

There are various methods of increasing the damping ratio of a structure. In cases where existing floors have vibrational problems, the addition of partitions either above or below the floor tends to increase damping to as high as 14% of critical [Allen (1974)]. For a planned structure, the use of non-composite construction tends to increase damping by 1-2% over composite construction. The use of damping posts, viscous dampers, TMDs, and active vibration absorbers is also possible.

Isolation of source

This form of vibration treatment is mainly concerned with steady-state vibrations caused by heavy machinery on a floor. There are various methods of isolating vibrating machinery, including heavy base blocks, rubber-in-shear mountings, air springs, and chemical grouting. It must however be noted that even where isolators are used, resonance between the disturbing force and the supporting structure should be avoided. For a more economical solution, the resonance effect could be avoided by a small alteration in the running speed of the machine [Steffens (1966)].

2.9 Recent developments

Finite element modelling of slab vibrations

The finite element method (FEM) of analysis was first introduced in the 1960s and its use has become widespread with the advent of faster and more efficient computer technology [Zienkiewicz (1992)]. The main feature of FEM is that it allows the division of a structure into many smaller components (elements) of various geometries which, when assembled together, can represent the whole structure. The assembled elements must not only reflect the shape of the structure but also ensure the correct flow of stress from the loaded zones to the reaction zones, hence the position of the nodes and the manner of their connection become very important [Carlton (1993)]. The steps involved in a typical finite element analysis are:

i) conversion of actual structure into an idealised structure

ii) conversion of the idealised structure into a geometrical model

iii) interpretation of the geometrical model as a meshed model of elements

iv) conversion of the meshed model into a mathematical model

v) running of the mathematical model to create a numerical solution

vi) using the numerical solution to perform a results interpretation

vii) characterisation of the behaviour of the real structure and the derivation of changes to the desired structural parameters, subject to the given loading conditions

The FEM can be used to model complex geometries easily and can solve problems which previously could be tackled only by the use of physical models or by prototype construction. It also allows a quick and inexpensive opportunity to evaluate several alternative solutions to a problem. In general, the use of the FEM can be categorised into four distinct applications: (1) prediction of complete structural behaviour, (2) verification of analytical methods, (3) comparison with experimental observation, and (4) in combination with theory, experiment and analytical results.

Reports of finite element investigations into the dynamics of floor slabs are few in number [Ellis and Ji (1996), Pavic et al. (1994), Pavic and Waldron (1996b), Ji and Ellis (1995), Zaman and Boswell (1996)]. Of these studies, most include a full experimental investigation coupled with a finite element model. The main drawback for the method is the level of accuracy of the final solution, which depends on the representation of the structure in terms of its boundary conditions,

material properties, geometry, and modelling of the excitation processes. If these factors in a model closely represent the actual conditions, then FEM can be the most accurate method of estimating structural response. The uncertainties involved in the representation of a structure by finite elements, and the moves to tackle the problem, are discussed briefly below.

With today's finite element systems and cost effective computing, the models being analysed are becoming increasingly complex with varying degrees of accuracy. However, until recently there were no means of coordinating the knowledge to achieve improved modelling of structures. To this end, the National Agency for Finite Element Methods and Standards (NAFEMS) was formed in 1983, which has developed a series of benchmarks for improved accuracy. The NAFEMS guidelines point out that an FEM is only as good as: (i) the model of the structure (mesh and elements), (ii) assumptions embedded in the properties used for each element, and (iii) the representation of the external loads and constraints in terms of the discrete boundary variables. For concrete or composite structures, the accuracy of an FE analysis can be influenced by the type of element used (solid, shell, plate), concrete and profiled decking material properties (Young's modulus and material strength), discontinuities within the structure (cracking, construction joints, support continuity), discrepencies between the design and actual values for slab thickness and concrete density, boundary conditions (fixed, pinned), and soil and foundation properties.

A major advantage of FEM is that it allows a structure to be modelled completely, hence giving a full set of solutions for a given loading function. For vertical floor vibration analysis, it would be wasteful in time and effort to model a whole structure when only the behaviour of a single component (e.g. a floor) is of interest. Hence, attempts have been made at modelling the floor by itself and introducing boundary conditions to represent the connections to columns, beams, etc. This technique has proved useful in some cases giving close estimates of dynamic behaviour.

Pavic and Waldron (1996b) and Reynolds et al. (1999) have investigated floor dynamics using FE model updating. This is a technique developed in the context of mechanical engineering, in which the output from an FE analysis is systematically correlated with test data and the system parameters tuned to optimise the agreement. They found that a pre-test FE model did not give a very close prediction of the actual floor behaviour, but when the model parameters were updated from experimental results, a very close estimate of floor response was possible. They concluded that the improvements to a dynamic FE model of a floor slab could be achieved by: (i) explicit modelling of columns (rather than the common practice of idealising columns as pin supports), (ii) explicit modelling of slab ribs (rather than approximation of the ribbed slab as an orthotropic structure), (iii) modelling deep beams as shell elements, and (iv) improvements on geometry, boundary condi-

tions, and material properties.

Hence, it can be concluded that FE modelling can be a very useful tool in the evaluation of floor dynamic behaviour, given correct idealisation of the structure. The experience gained in modelling one structure accurately will be invaluable in improving the accuracy of FE models of other floors. To this end, experimental data from dynamic testing are required to enable correlation with FE models. Ji and Ellis (1995) suggest that a combined theoretical and experimental study on the structure is important because an experimental study provides accurate but incomplete information (depending on variables measured), while a theoretical study supplies complete but potentially inaccurate results, which can be improved. The use of finite element modelling will become even more important in the future with increasing use of computer models in design [Ellis and Ji (1996)].

Active control approach for reducing floor vibrations

Active control technology is used in many disciplines to improve the response of dynamic systems. For instance, its application in the field of earthquake engineering is currently attracting major interest. Its usefulness in reducing floor vibrations has also been studied recently. Hanagan and Murray (1997) reported a successful implementation of such a system on a problematic floor slab.

In their control scheme, the movements of an experimental floor were measured and utilised in a feedback configuration to supply a control force that resulted in a reduction of vibration levels. The control force was supplied by an electromagnetic actuator mounted on the floor. Their experimental tests agreed well with the analytical studies and showed that for heeldrop excitation the floor damping increased from 2.2% to 9.7%. The damping became as high as 40% with less severe impulse forces, which were within the most useful range of the controller. In addition, walking excitation tests showed a reduction of peak velocity amplitudes to 12% of those recorded for the uncontrolled system.

While the experimental results are encouraging, the system has potential drawbacks, such as its disruptiveness to building functions, the complexity of its design, its control when in function, its high cost, and maintenance/reliability issues. Such systems are in their early stages of development and there is currently no record of their utilisation on real floors.

Chapter 3

Design and construction of experiment

3.1 Introduction

The objectives and nature of the research are stated in section 1.3. The purpose of this chapter is to describe the preparation phase of the laboratory tests. First, the design and building stages of the test apparatus are described. Casting of the model floor slab and the various non-structural additions are then explained. The calibration procedures and accuracy of the apparatus are checked in section 3.7. Discussion of the test procedures and data collection methods is given in Chapter 4.

3.2 Outline of tests

The overall layout of the experimental apparatus, used in the modal testing of the model floor, is shown schematically in figure 3.1. The sources of loading were in four forms: impulse hammer, electromagnetic shaker, a person performing heeldrop loading, and either walking horizontally or on the spot. For the hammer and shaker tests, the actual applied load was measured and recorded. The tests with human activities were attempted to be as representative to real-life loading as possible. The actual experimental procedures for each loading type are explained in detail in Chapter 4.

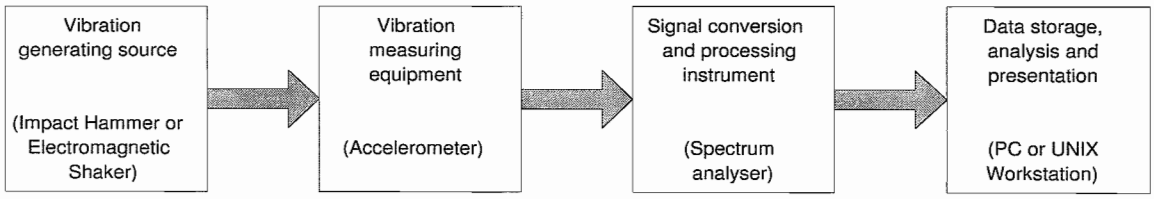

Figure 3.1: Layout of modal testing experiments on model post-tensioned slab

The slab response to each of the imposed dynamic loads was measured using a piezoelectric ac-

celerometer, which was placed in a closely spaced grid on the slab. The output of the accelerometer was amplified and recorded in a spectrum analyser, where data analysis was performed.

The model slab was designed as a 5.5×1×0.125m post-tensioned concrete slab with design concrete strength of 40N/mm^2, using Ordinary Portland Cement. The design was in such a way that the slab would represent a simple idealised one-way spanning floor, which could easily be altered and non-structural components easily fixed. Sufficient bonded steel was included to enable testing of the slab without any tensioning of the tendons. The tendons were then tensioned to 57% of their design stress, at which stage more tests were carried out, and finally to 100% of the design force. Once the model floor was post-tensioned to its full design stress, loading and response tests were carried out on the following slab stages: bare slab, slab with dead load, with partitions, with false floor, with standing human, with TMD, and with viscoelastic screed. Various combinations of these components were also investigated.

At regular intervals during the experimental investigation, cube and cylinder tests were carried out to determine the material properties of the concrete. In addition, 1500×200×150mm beams were cast and tested for the original slab concrete and the two viscoelastic screed layers.

3.3 Description and design of apparatus

The experimental apparatus consisted of two main elements: the loading equipment and the measurement instrumentation. Some items, for example the impulse hammer, are standard testing equipment developed previously by specialist firms. For other items, e.g. the shaker, specific design and modifications were necessary in order to adapt them to the requirements of the research programme. Details of individual testing apparatus and any necessary modifications form the bulk of the following sections.

3.3.1 Instrumented impact hammer

This instrument represents a relatively simple way of exciting the structure into vibration. The equipment consists of a 5.4kg impact hammer [Dytran Instruments Inc. (1993)] with a set of different tips for the head, which are used to vary the frequency and force level ranges. Integral with the impact head, there is a quartz piezoelectric force transducer, which detects the magnitude of the input force felt by the hammer head, assumed to be equal and opposite to that experienced by the structure. The hammer testing kit also includes a charge amplifier/power supply unit that

outputs the force signal at a level of 1V per 1000lbf (4448N). The magnitude of the impact force is determined by the mass of the hammer head and the velocity with which it is moving when it hits the structure. The frequency range of excitation is controlled by the stiffness and mass of the impact head. The stiffer the material, the shorter will be the duration of the pulse and the higher will be the frequency range covered by the impact. Figure 3.2 shows the hammer excitation equipment and figure 3.3(a) shows the frequency and magnitude ranges covered by each tip. With regards to concrete floor slabs, which exhibit low natural frequency, it is good practice to use a soft tip to input an impact of a shorter frequency range with more energy into the lower frequencies. For this research programme, different hammer tips were experimented and the brown tip made of polyurethane plastic was seen to be most suitable and was used throughout the testing programme. Figure 3.3(b) shows a typical hammer signal using the brown tip. The hammer testing procedure is described in chapter 4 and shown schematically in figure 4.4 on page 75.

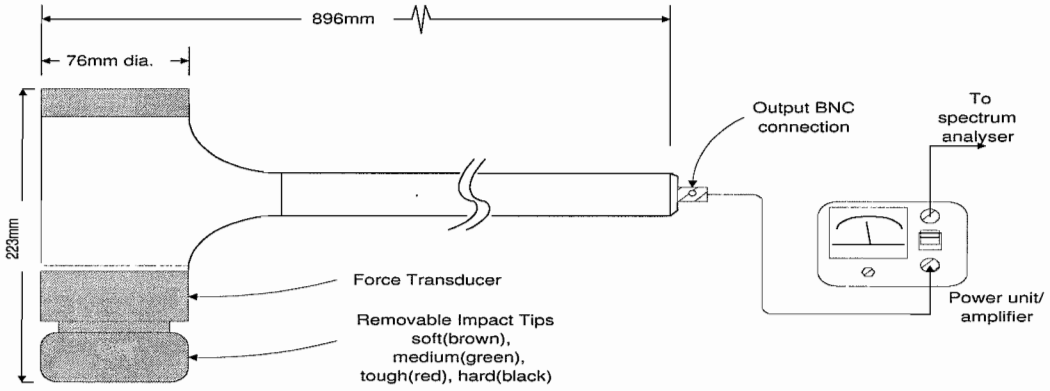

Figure 3.2: Instrumented impact hammer testing kit

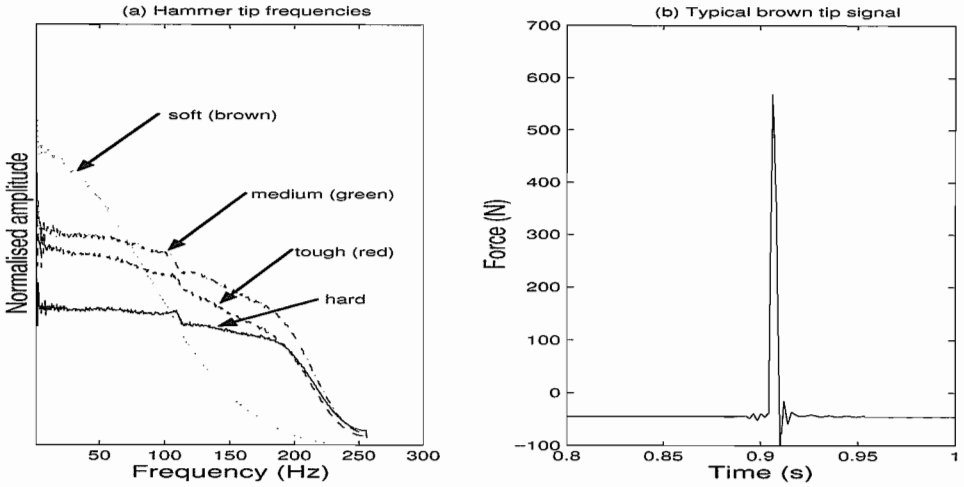

Figure 3.3: Frequency range and magnitude of impulse hammer tips and a typical hammer signal using the brown polyurethane tip

It is important to recognise that the impact hammer is only in contact with the structure for a short period while the excitation is being applied. This type of instrument is categorised as a non-contacting vibration source and imposes transient vibration on the structure. The contacting type of excitation is the shaker, which is described below.

3.3.2 Electromagnetic shaker

This type of excitation source is more bulky and is connected and remains attached to the structure throughout the test at all frequencies and amplitudes of excitation. It is categorised as a contacting source and imposes a continuous oscillation on the structure.

The electromagnetic shaker consists of a coil inside an electromagnetic field, whose input signal is supplied by an external signal generator. The coil in turn is connected to the drive part of the device, which is attached to the structure. In this case, the frequency and amplitude of the excitation are controlled independently of each other, giving more operational flexibility as compared to the impact hammer. It is hence possible to excite the floor at a particular frequency and obtain a more accurate response measurement at that frequency. As such, the results derived from a floor excited by a shaker have distinct advantages over those derived using an impact hammer [Falati (1996)].

The shaker used for this research programme was a Ling Dynamic Systems Vibrator model 410 [Ling Dynamic Systems Ltd. (1972)], which is capable of applying 178N through its drive head when force cooled by air. A 300W output valve power amplifier was used to amplify the signal from the signal generator on route to the shaker coil. A special frame was designed and built in order to carry the shaker and modify it for use in the research programme. This was a major part of the apparatus design and is explained in some detail below.

Design of shaker frame

The shaker, as supplied, was designed for horizontal applications or to be used in cases where the drive head was required to act upwards. Hence, a frame was designed and built in order to contain the shaker such that the drive head would be facing downwards and would be in contact with the floor slab continuously. As the shaker had a mass of approximately 30kg, a substantial frame was required to hold it in an inverted position and also to resist any movement upwards while it was operating. Figure 3.4 shows the designed frame with the shaker installed and individual components marked. A brief description of these is given below.

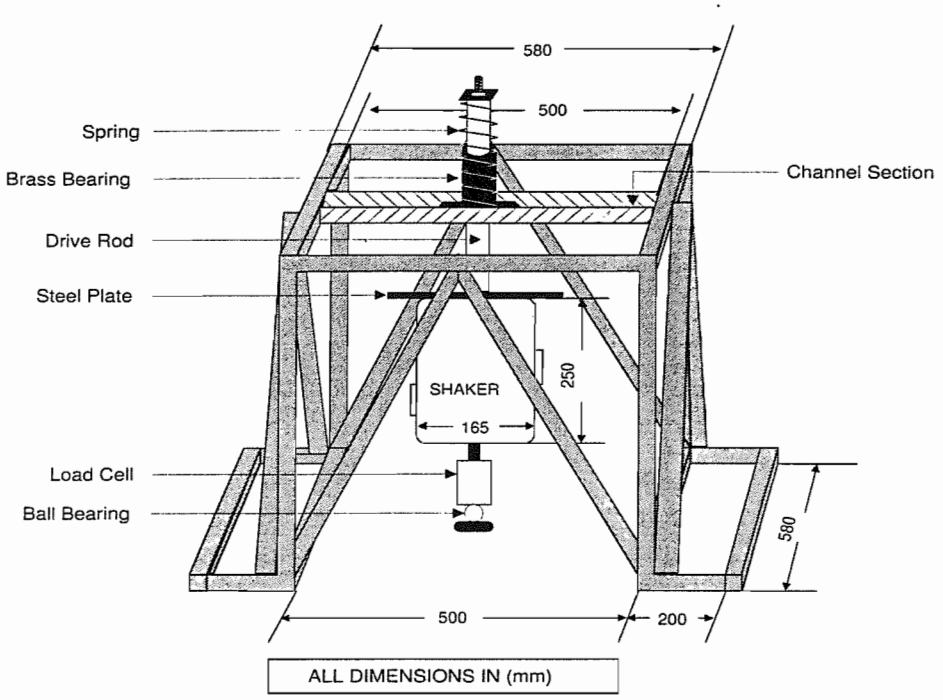

Figure 3.4: Electromagnetic shaker designed frame and its components

40mm Square Hollow Sections: Fillet welded together to construct the main frame.

500×76×38mm Channel Section: spanning the top of the frame to accommodate the brass bearing holding the shaker.

26mm diameter Brass Bush Bearing: consisting of a brass block which was machined to have a bearing of 26mm through which the rod holding the shaker would move.

25mm diameter Drive Rod: welded at bottom to a 13mm thick steel plate holding the shaker. The surface of the rod was constantly smoothed and lubricated for ease of movement through the bearing during shaker operation.

28.5mm diameter Compression Spring: resisting the weight of the shaker. The spring properties were: load capacity=1023N, spring constant=24.87N/mm, inside hole diameter=28.5mm, and free length=88.9mm. The height of the shaker and hence the compression of the spring could be altered by way of a nut at top of the drive rod.

13mm thick Steel Plate: welded at the top to the moving rod and at the bottom bolted to the shaker using fatigue resistant bolts.

1000N maximum capacity Load Cell: used to measure the force output of shaker drive head onto the floor (see section 3.3.4).

25mm diameter Ball-Bearing: joining the load cell to the floor via a steel base. Used for reducing error effects and preventing damage to the shaker due to lateral loading.

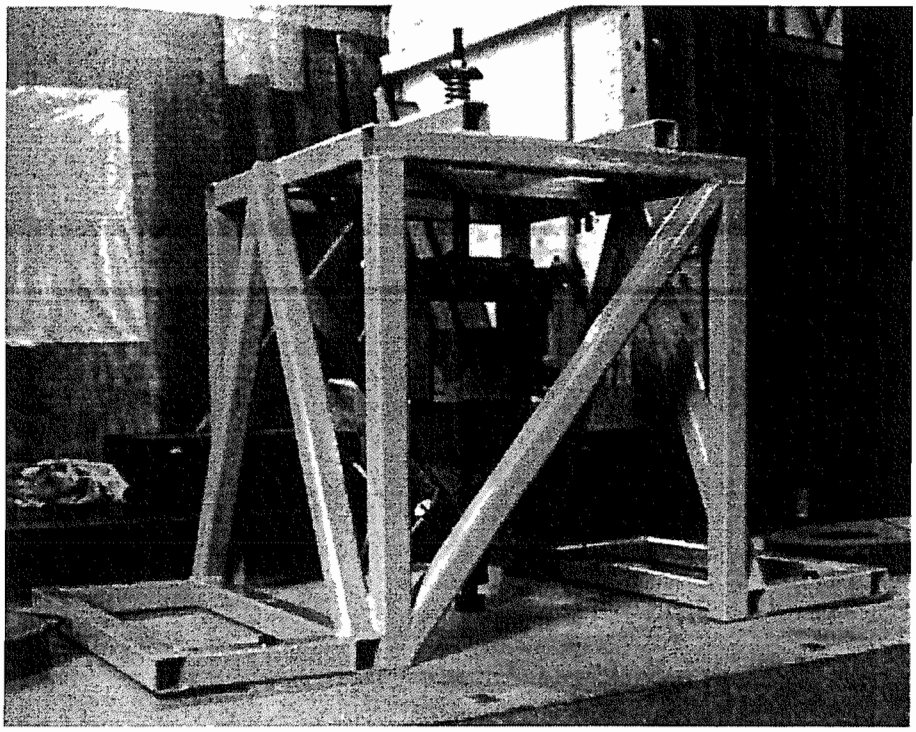

Figure 3.5: A view of the shaker frame and its components

In operation, an initial pre-compression of 50N was applied to ensure the ball-bearing was fully in contact with the floor. The shaker would then impose a continuous sinusoidal loading onto the floor and its subsequent upward motion would be resisted by the compression spring. The shaker frame, with the components installed, is shown in figure 3.5 and its experimental setup is explained in chapter 4. The test procedure is also shown schematically in figure 4.4 on page 75.

3.3.3 Piezoelectric accelerometers

The accelerometers used were model 4370 manufactured by Brüel&Kjær [Brüel&Kjær (1982)]. A B&K charge amplifier type 2635 was used and the acceleration signals were amplified to 1V per g. These signals were then fed into the spectrum analyser for initial frequency domain analysis. Piezoelectric accelerometers work on the basis that the piezoelectric material inside, usually quartz, generates a small electric charge in response to applied accelerations. Once amplified and calibrated, this signal can be used as a measure of acceleration response of the structure. Due to the sensitive nature of the accelerometers, the measured data was constantly monitored and the accelerometer sensitivities altered accordingly. Figure 3.6 shows the B&K accelerometers used in testing.

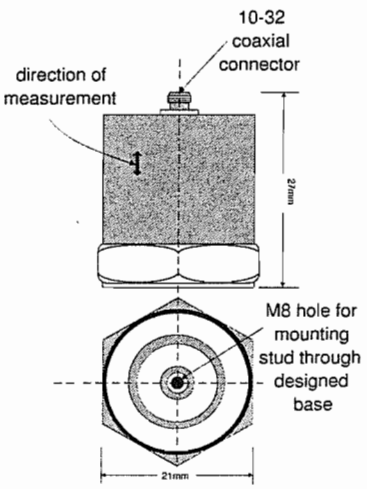

Figure 3.6: A schematic view of the B&K accelerometers used in the modal tests

3.3.4 Load cells

The load cell used for the shaker test was an external Wheatstone Bridge type 1000N ultimate capacity transducer manufactured by Schlumberger. It was placed between the shaker drive head and the floor and would measure the force exerted onto the slab. This load cell was powered by an RDP instruments E307 'black box' power supply. The electrical output of the transducer was amplified by the 'black box' and then fed to the spectrum analyser for time and frequency domain analyses. The load cell calibration procedure is described in section 3.7.2.

3.3.5 Spectrum analyser

The spectrum analyser used in the Oxford University civil engineering group is an Advantest model R9211C [Advantest Corp. (1989)]. This is a very powerful signal processor with signal generating capabilities. Both these parts of the analyser were utilised in the experimental programme.

The signal generating function was used to provide the sinusoidal wave forms which, after amplification, would be fed to the electromagnetic shaker and ultimately control the movement of the shaker drive head. The frequency, amplitude and type of the input signal could be controlled and altered independently. The signal processing capabilities of the spectrum analyser were widely used in the initial data analysis. As shown in figure 3.7, the equipment has two input channels. Channel A was connected to the output of the load cell, either from the hammer or shaker, and would provide the force information for the eventual transfer function. Channel B was connected to the acceleration transducer on the slab and would read the amplified acceleration response to the imposed force. Digital signal processing was carried out by the analyser and the results were

obtained in the form of a frequency response function (FRF) describing the relative magnitudes of the range of frequencies present in the signals. Also at this stage, the coherence function was checked and the accuracy of the experiment evaluated. The underlying theory of signal processing is presented in section 4.2.

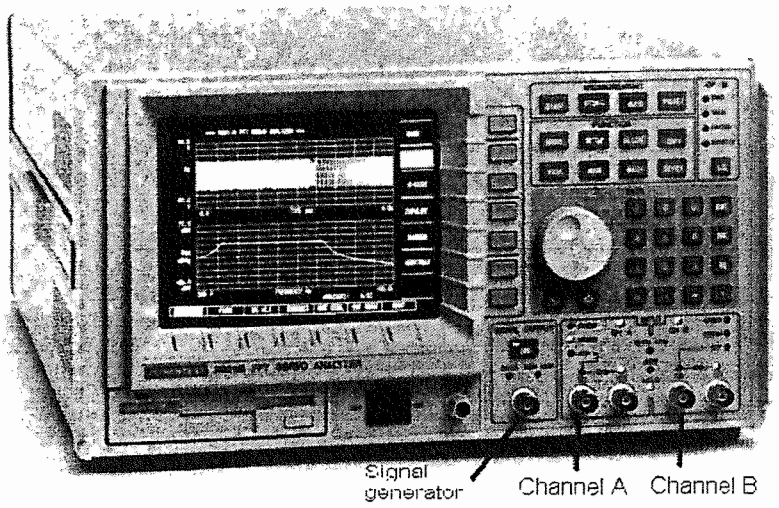

Figure 3.7: Advantest R9211C spectrum analyser

As the analyser was not equipped with an IEEE488/RS332 interface circuit, it was not possible to transfer the data directly to a computer for storage and further analysis. Hence, the data saving facility of the analyser was also very widely used, where the information was saved on floppy disks and subsequently transferred into a PC. Furthermore, as the analyser did not save the information in a *DOS* or *Windows* compatible format, a substantial amount of time was spent in converting the saved data from the analyser format to a format recognisable by a PC, using a translation program written in *QBASIC*.

3.4 Design of the model floor slab

3.4.1 Objectives of the design

Since the main purpose of the research programme was to investigate vibration problems of post-tensioned floor slabs due to resonance with human activity, it was essential that the test floor's fundamental natural frequency fell within one or more of the harmonics of man-induced excitation. For an effective experimental programme, the model slab must therefore posses a fundamental natural frequency in the range 2-9Hz. This became the first priority of the model slab design.

Only the most slender post-tensioned floors are likely to experience vibrational serviceability problems. Current construction practice is to use post-tensioning for spans in the range 7-20m, where solid slabs are used in the lower end of the range and waffle slabs used for longer floors. For solid slabs, thicknesses are usually 200-300mm, resulting in span-depth ratios between 30 and 45. Average prestress levels are typically 3-5MPa. All of these facts were taken into account to produce a realistic 50% scaled model post-tensioned floor.

Other priorities were: the concrete strength to represent real cases, post-tensioning tendons used, and the overall weight of the slab, which had to be below the safe working load of the laboratory lifting equipment.

3.4.2 Dimensions and limitations

In arriving at a suitable size for the experimental slab, the space available in the laboratory became the most important factor. The dimensions of the final design were 5.5m long by 1m wide and 125mm deep, giving an initial span-depth ratio of 44. Ideally, this gave a calculated fundamental frequency of 5.6Hz (using equation 2.8 on page 23), which was the lowest possible under the laboratory space limitations. After construction of the slab and its placement on the supports, the length between the supports became 5.1m with an average thickness of 135mm, giving a span-depth ratio of 38 and a fundamental frequency of 7.96Hz (see appendix D). This would mean that a condition of resonance could be achieved with the third harmonic of walking frequency. It would have been desirable to have had a longer and wider slab, exhibiting two-way spanning behaviour and lower fundamental frequency, but the laboratory conditions did not allow this.

3.4.3 Design of slab as a reinforced beam

After deciding the dimensions, the slab was designed in a reinforced and post-tensioned state. The design of the model floor as a reinforced beam was to ensure enough bonded steel was included in the concrete so that it would withstand its own self-weight without any tensioning of the pre-stressing tendons. The design followed the usual British Standards [BS8110 (1985)] specifications with the following design values and reinforcement bar sizes: f_{cu}=40N/mm^2, cover=20mm, f_y=460N/mm^2 and 10mm diameter reinforcement bars. The design dead load was 4.5kN/m^2 and the design live load was 3kN/m^2 to account for people standing on the slab.

3.4.4 Design of slab as a post-tensioned floor

The floor was designed as a flat slab according to BS8110 and with the guidelines specified in Concrete Society (1994). Prestress was provided by four 15.7mm diameter PSC Freyssinet unbonded super-strands, with a characteristic breaking load of 265kN and characteristic strength of 1770N/mm^2. The sheathing used for these tendons was of plastic type. The design eccentricity was 30mm.

The slab was designed as a Class 1 member with maximum tensile stress under service conditions f_t=0N/mm^2, and maximum service compressive stress f_{cc}=15N/mm^2. When fully stressed, each tendon provided a prestressing force of 175kN, giving an average prestress in the slab of 5.2MPa, which was high but within the acceptable range. Figure 3.8 shows the final reinforcement cage with the post-tensioning tendons included. Figure 3.9 shows photographs of the tendon anchors.

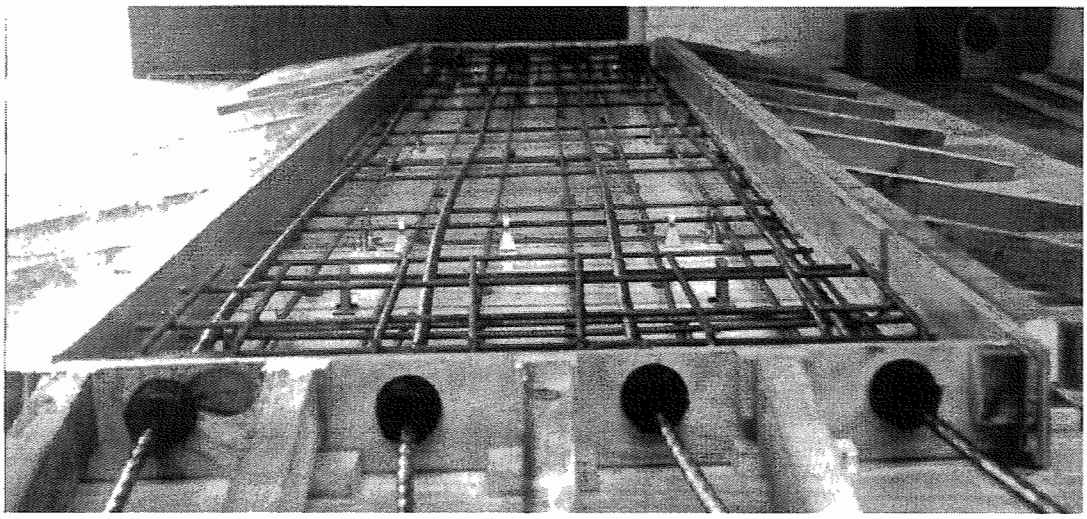

Figure 3.8: Reinforcement cage of model experimental slab showing the bonded steel and unbonded tendons

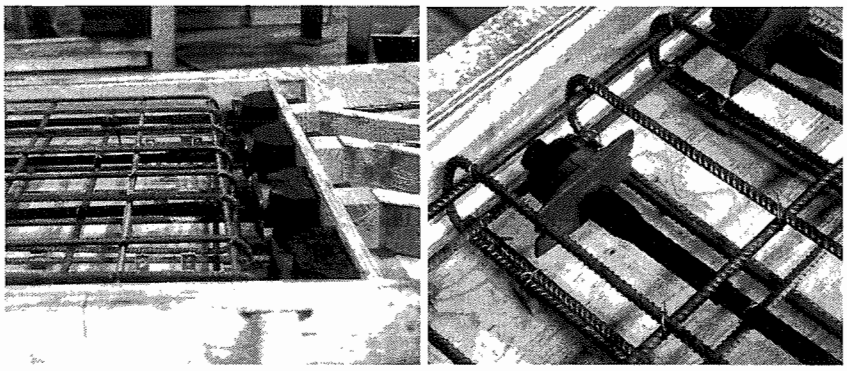

Figure 3.9: Details of live tendon anchors (left) and dead anchors (right)

3.4.5 Design of slab supports

In order to achieve as low a fundamental frequency as possible, simple supports were used at either end. These were in the form of 60mm diameter circular rods, which were welded to the top flanges of two 400mm deep steel girders. The height of the supports was deliberately large to allow access to the bottom of the slab for fixing partitions, as explained in section 3.6.3. The slab at either end would hence rest on the circular rods with a minimum point of contact, so that the rod acts as a line support. Figure 3.10 shows one of the designed simple supports with the slab resting on it via 3mm thick hard rubber sheets to eliminate uneven contact. The inclusion of the rubber did not affect the dynamic characteristics of the slab.

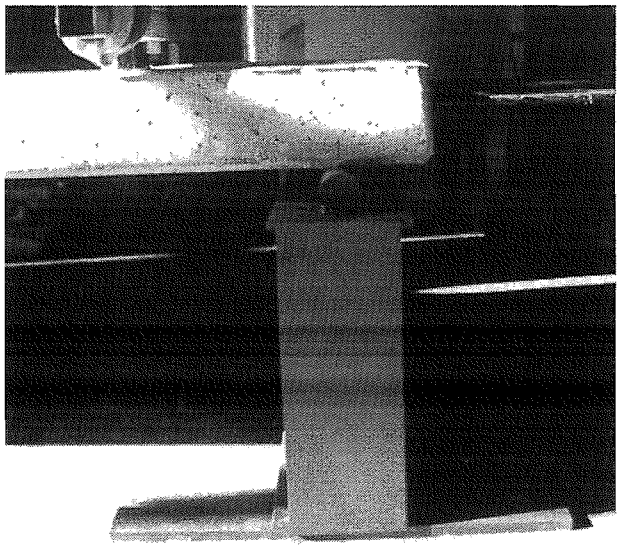

Figure 3.10: Simple supports used for experimental slab

3.5 Construction of the model floor slab

The dimensions of the experimental slab meant that 700 litres of concrete ($0.7m^3$) were required for its casting. In addition, small scale test samples had to be taken. The following sections describe the processes involved before and during the casting of the slab and other concrete samples.

3.5.1 Concrete mix design

The design concrete strength was $40N/mm^2$ with a permissible standard deviation of $3N/mm^2$. The density was taken to be $2400kg/m^3$ and the concrete was designed for a slump test of 50mm. The

mix quantities per cubic metre were: coarse aggregate 955kg, fine aggregate 750kg, cement(OPC) 432kg, and water 205kg. Small scale cube and cylinder samples of the mix were taken to check the design specifications against the eventual concrete properties.

3.5.2 Concrete casting process

Since the laboratory concrete mixer had a maximum capacity of 50l, needing 14 mixes, special priority was given to the speed of casting of each mix in order to avoid cold joints in the slab. The casting process involved 10 volunteers, three of whom were casting and vibrating the wet concrete, two were mixing, one taking small scale samples, two weighing the mix constituents, and the remaining two responsible for the transport of the wet concrete from the mixer, on ground floor, to the formwork, on first floor. Figure 3.11 shows the final result after completion.

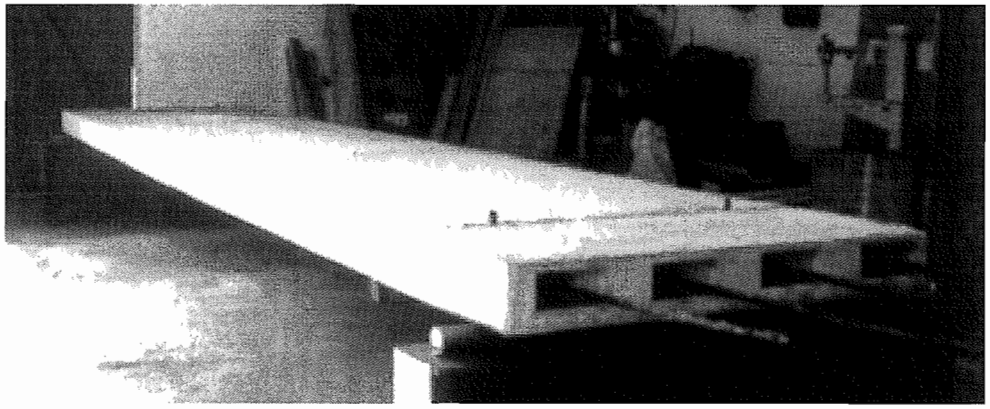

Figure 3.11: Model floor slab after curing

3.5.3 Small scale test samples

In total, 15 cubes of the mix were taken and two 300mm×150mm diameter cylinder samples were also cast. A further 10 cubes and 3 cylinders were cast in the latter stages of the experiment, which included the viscoelastic screed mixture (see section 3.6.7).

In addition, four small beams of 1500×200×150mm were cast during the whole of the experimental procedure. These consisted of two beams representing the concrete mixture used in the experimental slab, and the other two representing the concrete mixture used for the viscoelastic screed layers. The beams were designed only to support their own self-weight and although they were doubly reinforced, the compression reinforcement was kept to a minimum and was only included to ensure safety during their movement.

3.6 Additions to the floor during testing

The following sections describe the various simulated non-structural components, which were added to the bare concrete, and the way each one was connected to the slab for testing.

3.6.1 Dead load on floor

The purpose of this addition was to simulate office furniture, which would be stationary on the floor, such as desks, cabinets, etc. Five 25kg Lead weights were used, which were placed at one meter spacings giving a notional dead-load of approximately 250N/m^2. The deflection of the slab due to this load was also measured.

3.6.2 Cantilever partitions

To simulate cantilever partitions, typical of those used to divide open-plan office space, three layouts were used. Firstly, five 9mm thick by 1.2m high gypsum plaster sheets were fixed perpendicular to the slab span at one meter spacings. Secondly, three sheets were installed parallel to the slab span, and thirdly, all eight were attached on the slab in both directions. 25mm equal sided steel angle sections were used to connect the cantilever sheets to the slab. The connection was made rigid by screwing angles on each side of the plaster sheets and bolting them together, and to the slab, while sandwiching the plaster in-between. Figure 3.12 shows an overview of the partition arrangement and figure 3.13 shows the slab with the first layout attached.

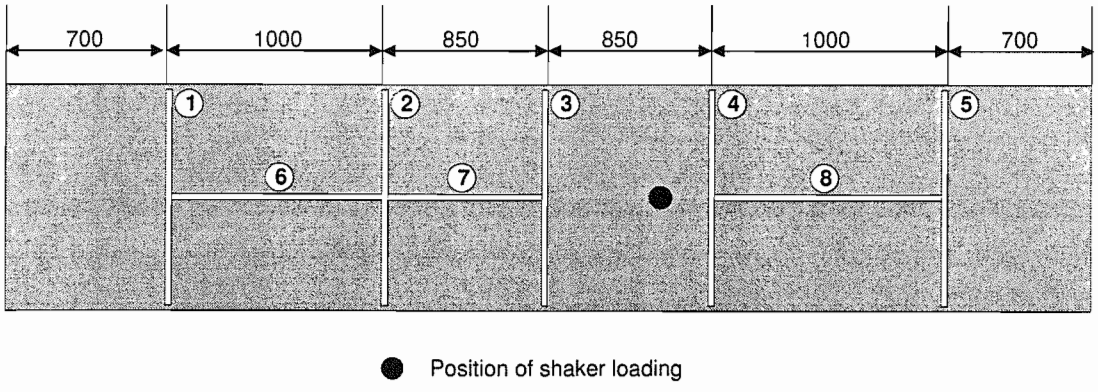

Figure 3.12: Layout of cantilever partitions on model slab

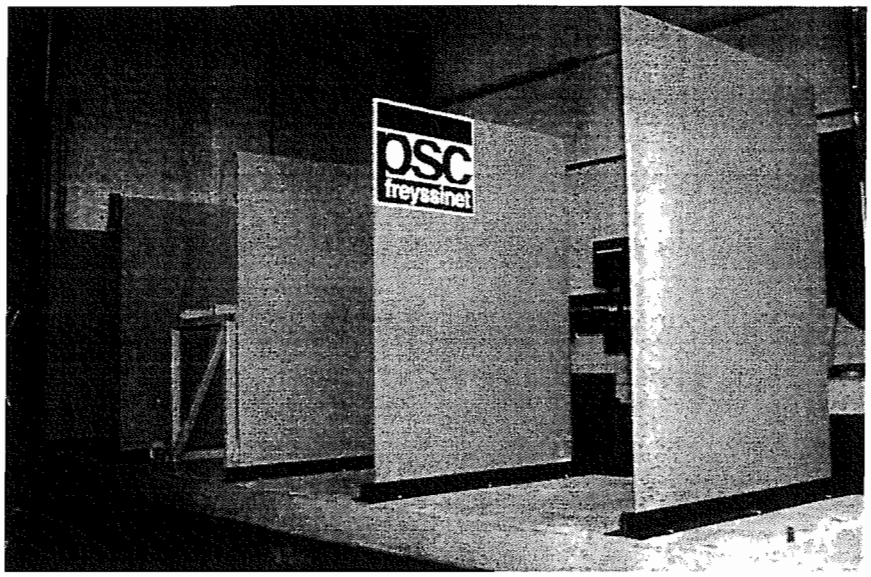

Figure 3.13: Experiments with simulated cantilever partitions

3.6.3 Full-height partitions

As for cantilever partitions, 9mm thick Gypsum plasterboard was used for the full-height partitions with the difference that both ends of the partitions were rigidly fixed, one to the bottom of the slab and the other to the ground. The fixing to the slab was made possible by the use of cast-in sockets, on the underside of the floor, and 25mm square steel angle sections. The bottom of these partitions were rigidly fixed to the ground using angle sections, which were glued on one side to the ground and bolted to the plasterboard on the other. Figure 3.14 shows the slab with full-height partitions attached.

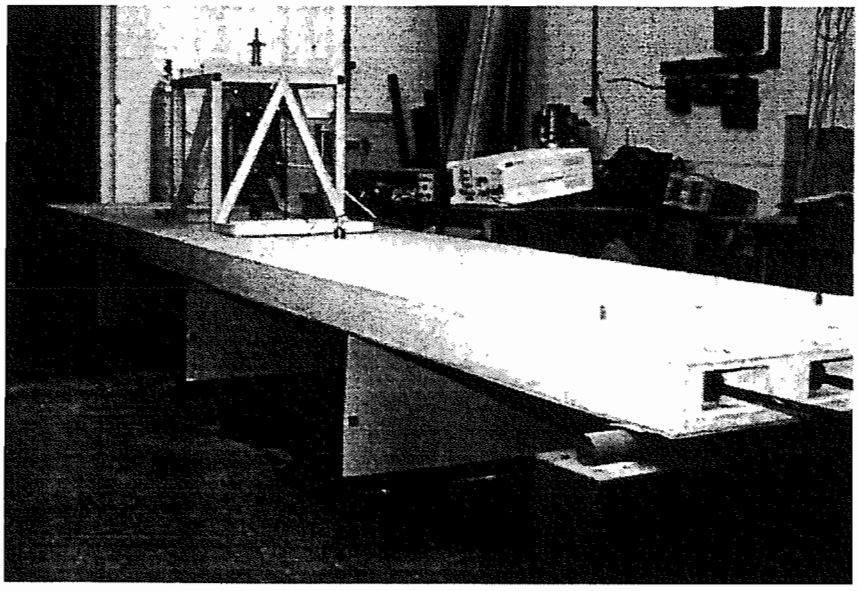

Figure 3.14: Experiments with simulated full-height partitions

3.6.4 False flooring system

The false flooring system used for the experiments consisted of 150mm adjustable height pedestals with adhesive for fixing to the floor, and a number of basic 600mm square false flooring panels, with a mass of 11.5kg each. These were fixed to the bare slab in two separate layouts. Layout 1, shown in figure 3.15, consisted of one row of 7 panels, covering around 50% of the entire floor, which were rigidly fixed to the pedestals on all four corners using special screws. This is a common mode of installation of floor panels. In layout 2, two rows of 7 panels were used, covering approximately the entire floor (see figure 3.16). Panels were screwed down at all interior corners but at the outer edge of the group, they simply rested on the pedestals. This gave some scope for relative movement between panel and pedestal during vibration testing. This detail is commonly used for panels around the edge of a floor or for heavy timber panels.

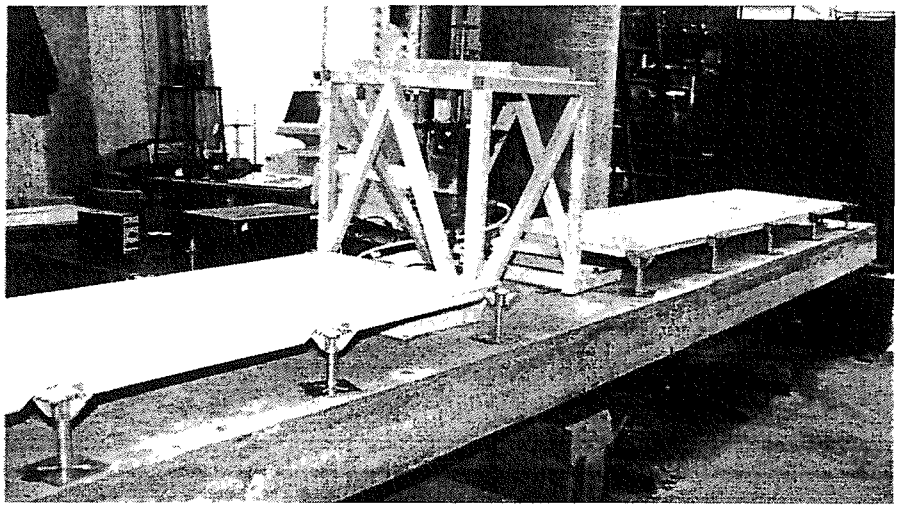

Figure 3.15: False floor panels layout 1

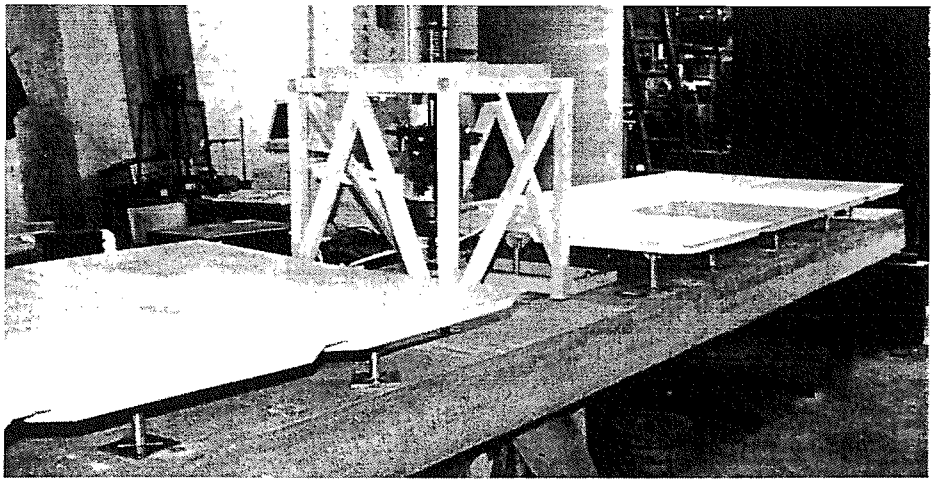

Figure 3.16: False floor panels layout 2

3.6.5 Tuned mass damper (TMD) system

To produce a TMD system for the experimental slab, cast-in sockets in the bottom of the slab were utilised to which 25mm square angles were fixed. A 1200mm long sheet of plywood was then placed in the space between the angles and rested on either side on the horizontal angle face. The TMD tuning effect was achieved by placing different weights on top of the plywood sheets. This experiment was performed with two different widths of plywood and also with single and double layers of plywood separated by polythene and rubber, as described in chapter 7. Figure 3.17 shows the slab with the TMD system attached.

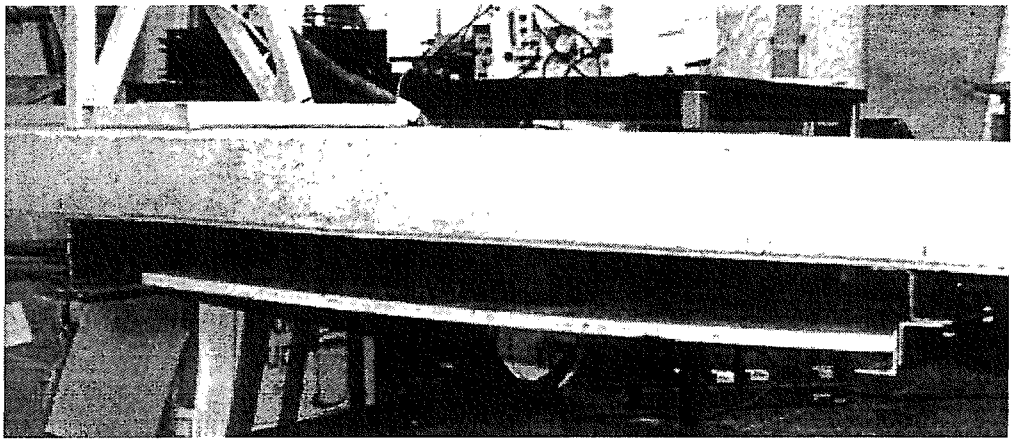

Figure 3.17: Application of TMD on slab

3.6.6 Standing human

Here, the effect of human-structure interaction was investigated, as described in chapter 8. A person of mass 75kg stood still on the bare slab during these tests. The position of the standing human was as near to the middle of the slab as possible. Figure 3.18 shows a test in progress with the human on the slab. Heeldrop, walking on-spot, and horizontal walking tests were also performed on the slab, as well as tests with two standing men.

3.6.7 Viscoelastic screed layers

This addition to the experimental slab was the only one which was irreversible and hence could be regarded as structural, rather than non-structural. It consisted of a 25mm layer of concrete, treated with a viscoelastic material, being added on top of the slab. Two layers of such additions were applied using different concentrations of viscoelastic additive. The viscoelastic material used was

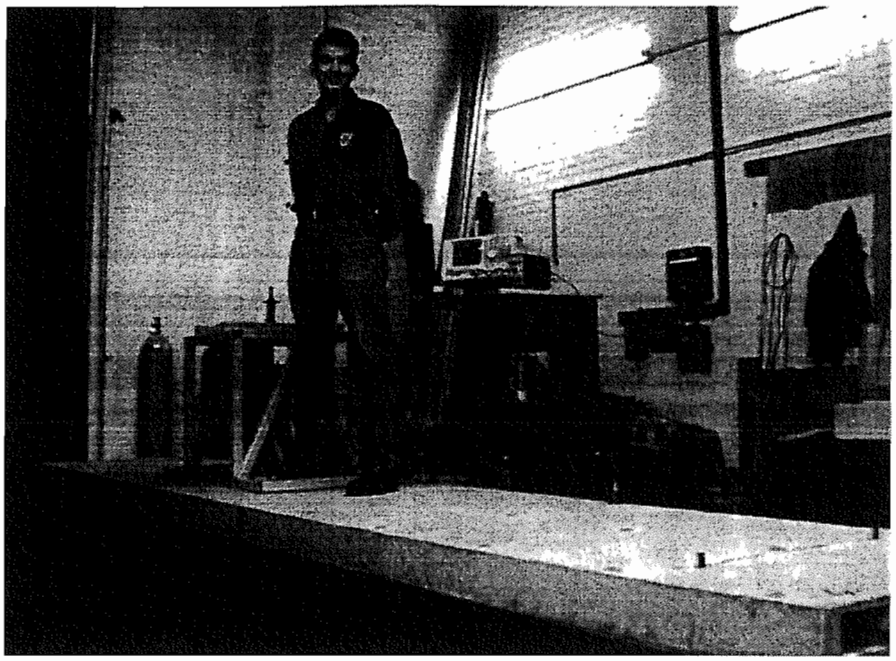

Figure 3.18: Experiments with one stationary standing man

donated by Concredamp Inc. (1993). This a patented additive and details of its constituents are not publicly available. The following two sections describe the preparation of the layers of concrete treated with Concredamp.

Concredamp Mix Design

The concrete mix design used for the Concredamp layers was exactly the same as the one used for the main slab with the difference that the amount of water in the mix was reduced by 50% of the amount of Concredamp added. This was according to the specifications supplied by Concredamp Inc. The two layers were cast at an interval of approximately one month and the concentrations of Concredamp used were $50l/m^3$ and $85l/m^3$ respectively.

Concredamp casting process

This was similar to the casting process of the main slab concrete, explained in section 3.5.2. The first attempt at layer 1 was abandoned after a period of ten days, when it was observed that the new layer had not achieved a good bond with the main concrete slab. This layer was subsequently removed and at the second attempt a better adhesion between the layer and the slab was achieved. In each case, it was noticed that the Concredamp additive had very adhesive behaviour (rather like paint) and had the effect of reducing the workability of the concrete mixture very quickly, making

the speed of casting more critical. Figure 3.19 shows the slab with two layers of screed added. In each case, screws were used as studs on the main slab to act as shear connectors and aid bonding.

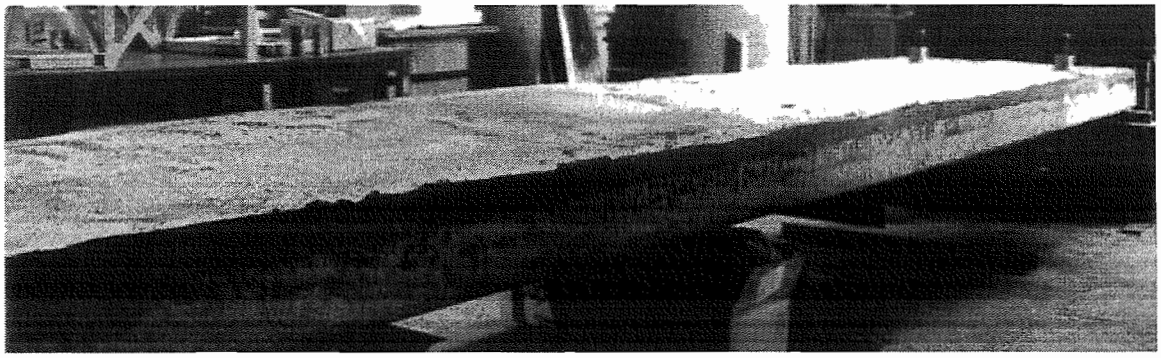

Figure 3.19: Slab with both layers of viscoelastic screed added

3.6.8 Some combinations

With the viscoelastic screed in place, it was possible to repeat the experiments with some combinations of slab additions. For example, tests were repeated with the screed layers and cantilever partitions or false floors and with standing human.

3.7 Accuracy of measurement systems

During the course of the experiments, it was necessary to check the reliability of the transducers involved, in order to ensure the accuracy of the measured data. The following sections give a brief description of the calibration and checking of the transducers.

3.7.1 Accelerometers

Each accelerometer was supplied with a detailed calibration certificate, which was used in the initial calibration of the experimental results. However, a simple way of checking the accelerometers was to put them alongside each other and to plot a transfer function of their respective outputs. A straight horizontal transfer function would mean that both accelerometers give the same output. This test was repeated at regular intervals during the testing program. Typical transfer function and phase plots of such a test are shown in figure 3.20, which were deemed to be acceptable.

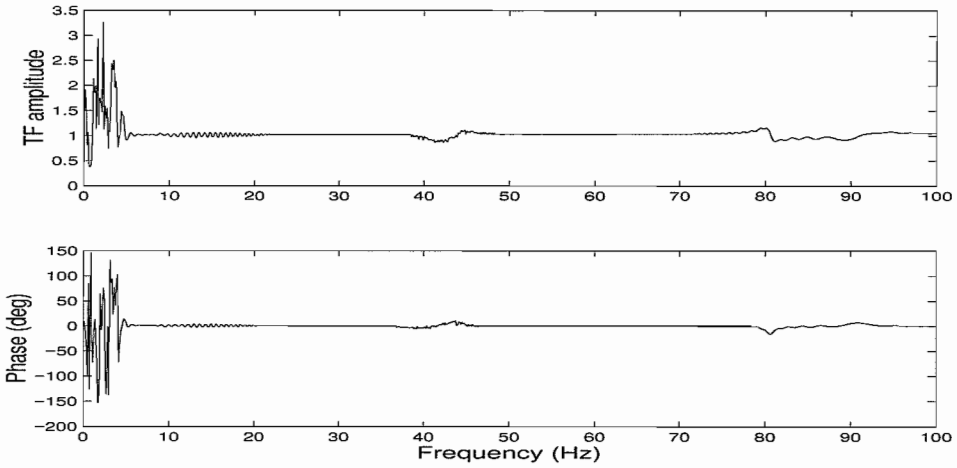

Figure 3.20: Transfer function and phase plots between two accelerometers

3.7.2 Load cells

Of the two load cells used, the one supplied integral to the hammer head had a factory calibration certificate, which was used throughout the experimental programme. The Wheatstone bridge load cell, however, had to be calibrated. This process involved putting known weights on top of the load cell and reading its output as a voltage. The applied load was increased in equal and unequal increments and the voltage plotted. The plot, as illustrated in figure 3.21, shows a linear increase in output voltage with added weight and hence this was used as the calibration plot for the load cell. This process was repeated in the middle and latter stages of the experimental programme with a similar calibration graph in each case.

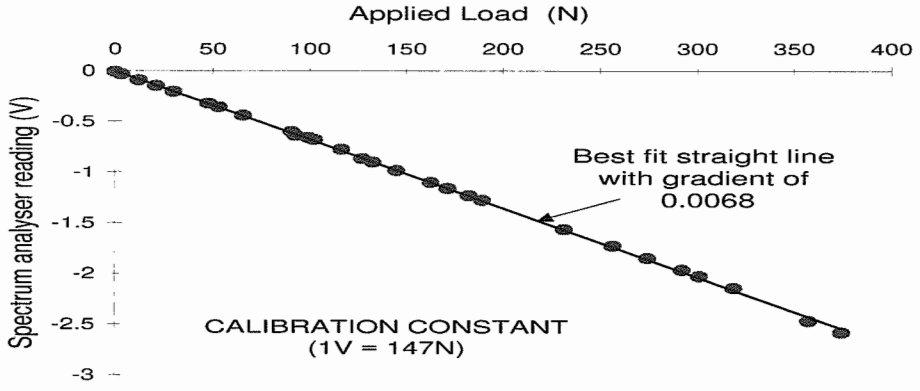

Figure 3.21: Calibration graph for the shaker load cell

3.7.3 Shaker loading

Here, it was desirable to see whether the sine-sweep loading, applied by the shaker onto the slab, closely simulated the sine-sweep signal produced by the signal generator. A transfer function was plotted between the signal processor wave-form and the output of the load cell attached to the drive head of the shaker. A straight horizontal line would mean a perfect representation of the wave by the shaker, whereas any deviations would signal an error at that particular frequency. Figure 3.22(c) shows a typical transfer function, which is satisfactory for frequencies above 6Hz and unsatisfactory for all lower frequencies. This was deemed acceptable for the purposes of this experiment, as the frequencies of interest were above 7Hz. Any noise in the signal was attributed to the loadcell readings and speed of data capture, neither of which were seen to affect the final results. This checking process was repeated throughout the course of the testing programme.

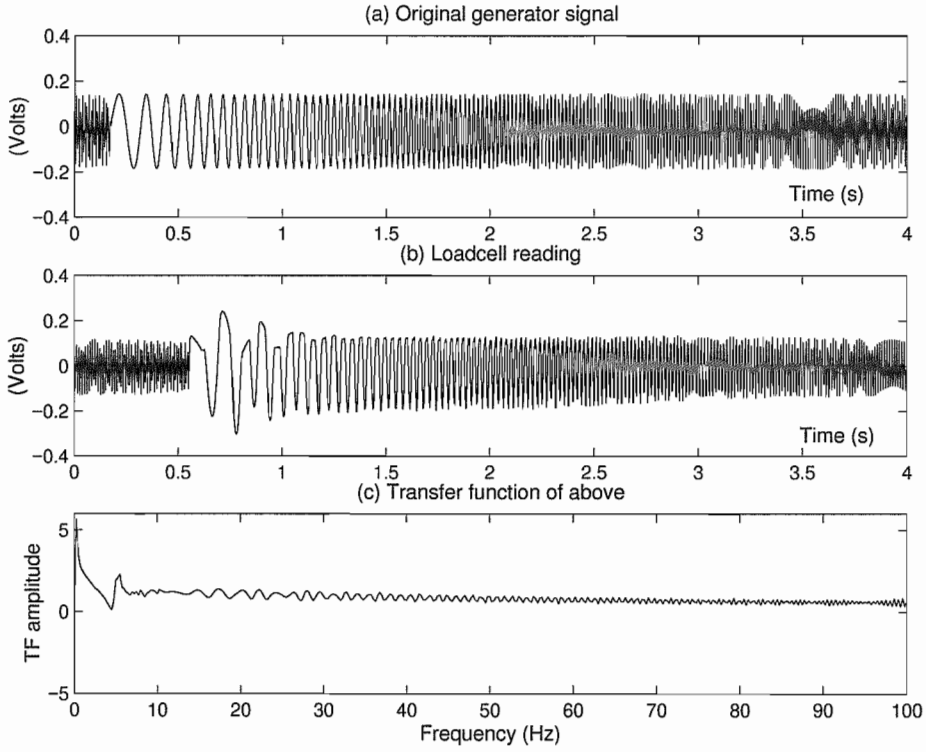

Figure 3.22: Accuracy of shaker loading compared with original signal